Article

Cell Reports

Intracellular *Mycobacterium tuberculosis* Exploits Multiple Host Nitrogen Sources during Growth in Human Macrophages

Graphical Abstract

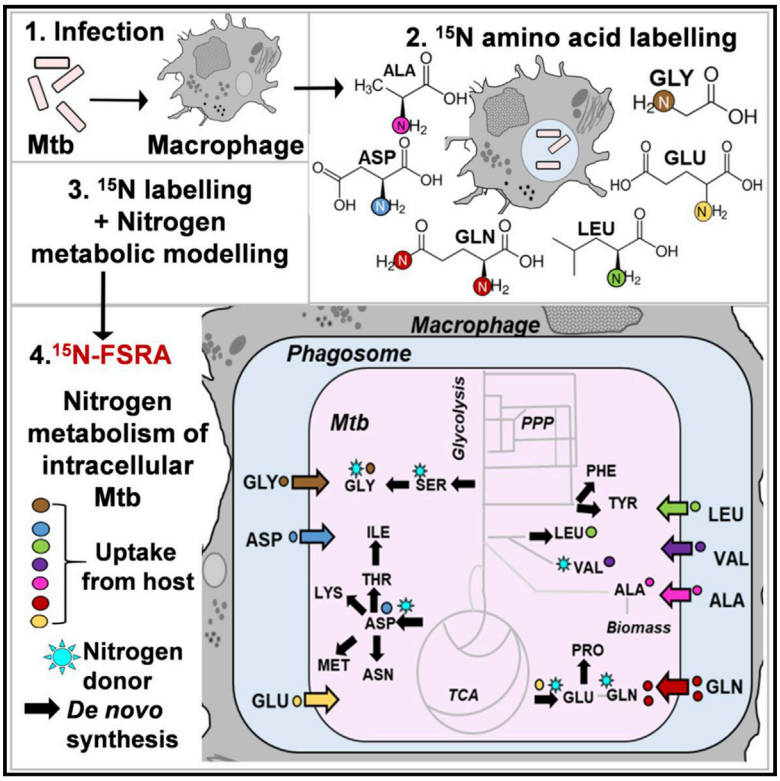

Highlights

- *Mycobacterium tuberculosis* utilizes multiple amino acids as nitrogen sources in human macrophages
- ^{15}N-FSRA tool identified the intracellular nitrogen sources
- Glutamine is the predominant nitrogen donor for *M. tuberculosis*
- Serine biosynthesis is essential for the survival of intracellular *M. tuberculosis*

Authors

Khushboo Borah, Martin Beyß, Axel Theorell, ..., Katharina Nöh, Dany J.V. Beste, Johnjoe McFadden

Correspondence

j.mcfadden@surrey.ac.uk

In Brief

Borah et al. measured nitrogen uptake and assimilation in *Mycobacterium tuberculosis* during replication in host macrophages using ^{15}N-flux spectral ratio analysis (^{15}N-FSRA), a systems-based tool. The biosynthetic and transport systems of the identified nitrogen sources involved in serine biosynthesis are potential drug targets.

Borah et al., 2019, Cell Reports *29*, 3580–3591
December 10, 2019
https://doi.org/10.1016/j.celrep.2019.11.037

CellPress

OPEN ACCESS
CellPress

Cell Reports
Article

Intracellular *Mycobacterium tuberculosis* Exploits Multiple Host Nitrogen Sources during Growth in Human Macrophages

Khushboo Borah,[1] Martin Beyß,[2] Axel Theorell,[2] Huihai Wu,[1] Piyali Basu,[3] Tom A. Mendum,[1] Katharina Nöh,[2] Dany J.V. Beste,[1,4] and Johnjoe McFadden[1,4,5,*]

[1]Faculty of Health and Medical Sciences, University of Surrey, Guildford, GU2 7XH, UK
[2]Forschungszentrum Jülich GmbH, Institute of Bio- and Geosciences, IBG-1: Biotechnology, 52425 Jülich, Germany
[3]School of Veterinary Medicine, University of Surrey, Guildford, GU2 7AL, UK
[4]These authors contributed equally
[5]Lead Contact
*Correspondence: j.mcfadden@surrey.ac.uk
https://doi.org/10.1016/j.celrep.2019.11.037

SUMMARY

Nitrogen metabolism of *Mycobacterium tuberculosis* (Mtb) is crucial for the survival of this important pathogen in its primary human host cell, the macrophage, but little is known about the source(s) and their assimilation within this intracellular niche. Here, we have developed ^{15}N-flux spectral ratio analysis (^{15}N-FSRA) to explore Mtb's nitrogen metabolism; we demonstrate that intracellular Mtb has access to multiple amino acids in the macrophage, including glutamate, glutamine, aspartate, alanine, glycine, and valine; and we identify glutamine as the predominant nitrogen donor. Each nitrogen source is uniquely assimilated into specific amino acid pools, indicating compartmentalized metabolism during intracellular growth. We have discovered that serine is not available to intracellular Mtb, and we show that a serine auxotroph is attenuated in macrophages. This work provides a systems-based tool for exploring the nitrogen metabolism of intracellular pathogens and highlights the enzyme phosphoserine transaminase as an attractive target for the development of novel anti-tuberculosis therapies.

INTRODUCTION

Tuberculosis (TB) is one of the top 10 causes of morbidity and mortality in the human population, responsible for 1.6 million deaths and 10 million new infections every year (WHO, 2018; Flynn, 2006; Zumla et al., 2013). The causative agent of TB, *Mycobacterium tuberculosis* (Mtb), primarily resides within the hostile environment provided by the phagosome of macrophages and can therefore resist stress conditions such as low pH, hypoxia, reactive oxygen species, reactive nitrogen species, and nutrient starvation (Gouzy et al., 2014a; Russell, 2001; Rustad et al., 2009). Metabolism within this restricted niche is key to the survival and pathogenesis of Mtb (Beste et al., 2011; Ehrt and Rhee, 2013; Eoh et al., 2017; Warner, 2014). Understanding Mtb's metabolism within the macrophage has therefore become an important focus for research, with the aim of identifying vulnerable metabolic pathways that could be targeted with drugs. Carbon metabolism in Mtb has been intensively investigated, and host-derived lipids, cholesterol, and CO_2 have been identified as essential nutrients for intracellular growth and survival of TB in animal models (Beste et al., 2011, 2013; Ehrt et al., 2018; Eisenreich et al., 2010; Gouzy et al., 2014b; McKinney et al., 2000; Niederweis, 2008; Schnappinger et al., 2003). Our ^{13}C-flux spectral analysis (^{13}C-FSA) approach, applied to the intracellular carbon metabolism of Mtb, also demonstrated that several nonessential amino acids are acquired by Mtb from macrophages, highlighting their availability as potential nitrogen sources within the human host. However, the identity of the primary nitrogen sources for intracellular Mtb remains uncertain. Amino acid acquisition and metabolism is important for the pathogenesis of several intracellular bacterial pathogens, including Mtb (Das et al., 2010; Eylert et al., 2008; Gouzy et al., 2013, 2014c; Kloosterman and Kuipers, 2011). For example, *Salmonella enterica*, *Serovar typhimurium*, and *Streptococcus pneumoniae* require arginine for intracellular survival and virulence (Das et al., 2010; Kloosterman and Kuipers, 2011), demonstrating that this amino acid is a nitrogen source. *Listeria monocytogenes* has been shown to acquire aspartate, alanine, and glutamate from the host macrophages for *de novo* amino acid synthesis (Eylert et al., 2008). Isotopologue profiling studies also identified the amino acid serine as a carbon and energy source for the growth and replication of *Legionella pneumophilia* (Eylert et al., 2010).

In vitro, Mtb can utilize a wide range of carbon sources but was only able to utilize 13 out of 95 tested compounds as nitrogen sources (Lofthouse et al., 2013). These included mainly the following amino acids: alanine, asparagine, aspartate, valine, glutamate, glutamine, ornithine, and serine. Agapova et al. (2019) recently extended this list to include arginine, isoleucine, and proline, and urea has previously been shown to be utilized as a nitrogen source *in vitro* (Lin et al., 2012). The work by Agapova et al. (2019) also demonstrated that growth rates and yields are higher when Mtb grows with amino acids, as compared with ammonium as nitrogen sources, and that like carbon sources, Mtb can co-metabolize two amino acids simultaneously *in vitro*. However, a comprehensive study to

identify the nitrogen sources for intracellular Mtb growing within the host macrophage has never been performed.

The Mtb genome encodes several transporters for both inorganic and organic nitrogen compounds (e.g., ammonium chloride [Amt] and nitrate [NarK2]), as well as ATP-binding cassette (ABC) amino acid transporters (Cole et al., 1998). Aspartate and asparagine have been detected in the Mtb phagosome, highlighting these amino acids as potential intracellular nitrogen sources. However, while the gene directing the transport of aspartate (AnsP1) was essential for the synthesis of nitrogen-containing compounds in a murine model of TB, this gene was dispensable for intracellular survival, suggesting that aspartate is not the primary nitrogen donor for Mtb growing within macrophages. Conversely, a study by the same group demonstrated that the asparagine transporter (AnsP2) was required for surviving intra-phagosomal acid stress but was dispensable for *in vivo* survival (Gouzy et al., 2013, 2014a). Glutamate dehydrogenase (GDH), the enzyme that catalyzes the production of glutamate from 2-oxoglutarate, is also essential for the intracellular survival of Mtb (Cowley et al., 2004; Gallant et al., 2016; Viljoen et al., 2013). However, GDH is also required for resistance to acidic and nitrosative stress in *Mycobacterium bovis* (BCG); therefore, the role of glutamate as a nitrogen source is uncertain. Mtb auxotrophic mutants of leucine, proline, tryptophan, and glutamine have previously been shown to be severely attenuated *in vivo* (Hondalus et al., 2000; Lee et al., 2006; Smith et al., 2001), indicating that biosynthesis of these amino acids is required by Mtb growing in the intracellular environment. Several other auxotrophic mutants (e.g., methionine, isoleucine, or valine) can, however, successfully proliferate in macrophages, indicating that these amino acids can be acquired from the macrophage milieu (Awasthy et al., 2009; McAdam et al., 1995). Mutagenesis studies are useful in identifying Mtb genes required for nitrogen uptake or metabolism during intracellular or *in vivo* survival; however, none of these studies have directly measured the uptake and assimilation of nitrogen by intracellular Mtb.

Isotopic tracer studies, combined with direct interpretation of the labeling patterns in metabolites, have emerged as a powerful strategy to study the intracellular metabolism of important pathogens (Buescher et al., 2015; Eylert et al., 2010). We previously used ^{13}C isotopomer analysis and developed ^{13}C-FSA to identify the intracellular carbon sources for Mtb (Beste et al., 2013). However, this approach was unsuitable for the current study because of the lack of backbone rearrangements in the metabolic network, as compared to carbon, and limited mass isotopomer information from single nitrogen atoms. To overcome these limitations, here we developed ^{15}N-FSRA, a computational platform for analysis of the uptake of all potential amino acids as nitrogen sources. Specifically, to counteract the limited measurement information, an array of ^{15}N labeling experiments was conducted under equal conditions, which was simultaneously evaluated in an integrative system-based approach. This work showed that Mtb uptakes and co-metabolizes multiple intracellular sources of nitrogen when replicating within its human host macrophage. These results identify amino acid metabolism as a target for TB therapeutics while also providing a systems-based tool that can be applied to study the nitrogen metabolism of other intracellular organisms.

RESULTS

Mtb Co-assimilates Multiple Nitrogen Sources during Intracellular Growth

To measure the uptake and assimilation of nitrogen during the intracellular growth of Mtb, THP-1 human macrophages were infected with Mtb in the presence of a ^{15}N tracer—aspartate (Asp), glutamate (Glu), glutamine (Gln), leucine (Leu), alanine (Ala), or glycine (Gly)—for 48 h, the isotopic steady-state labeling period established in our previous work (Beste et al., 2013). Asparagine was not tested, as it had previously been shown to be a nitrogen source for intracellular Mtb (Gouzy et al., 2014a). Proteinogenic amino acids were used for isotopomer analysis because they acquire the labeling pattern of their central metabolic precursors and are abundant and stable (Beste et al., 2013) (Figure S1, I). Using an identical method to that developed by Beste et al. (2013), macrophage and Mtb fractions were separated, and ^{15}N incorporation into proteinogenic amino acids from infected macrophages and intracellular Mtb was measured using gas chromatography-mass spectrometry (GC-MS). Amino acid pairs of glutamate, glutamine and aspartate, asparagine (Asn) cannot be distinguished using GC-MS due to acid hydrolysis, so the ^{15}N enrichments for these amino acid pairs are combined as glutamate/glutamine (Glu/n) and aspartate/asparagine (Asp/n), respectively. Experimental controls of uninfected THP-1 macrophages and *in-vitro*-grown Mtb were cultivated in Roswell Park Memorial Institute (RPMI) containing each of the tracers for 48 h. These experiments established that the ^{15}N labeling profile of proteinogenic amino acids from intracellular Mtb was distinct from that of Mtb in RPMI (Figures 1C and S1, II). For example, the labeled nitrogen from $^{15}N_1$-Leu was incorporated predominantly into Leu when Mtb was tested in RPMI, but it was widely dispersed into other amino acids for Mtb growing intracellularly (Figure S1, IID). Similarly, for Mtb in RPMI, the label from $^{15}N_1$-Asp, $^{15}N_1$-Glu, and $^{15}N_2$-Gln was incorporated into Asp/n and Glu/n. However, during intracellular growth, labeled nitrogen from $^{15}N_1$-Asp was incorporated into almost all measured amino acids, including Asp/n and Glu/n (Figures S1, IIA–IIC). The distinct ^{15}N labeling profiles of intracellular Mtb versus *in-vitro*-grown Mtb in RPMI demonstrated that there was negligible cross-contamination from extracellular Mtb in these experiments. Moreover, there was no cross-contamination during the separation of the macrophage and the intracellular Mtb, as evidenced by the unique labeling profile of proteinogenic amino acids from these two fractions (Figures 1A and 1C). The labeling profiles of proteinogenic amino acids from infected and uninfected macrophages were virtually identical, indicating that Mtb infection does not significantly perturb the nitrogen metabolism of macrophages (Figures 1A and 1B).

In accordance with expectations, most of the amino acids derived from macrophages remained unlabeled, reflecting their direct uptake from unlabeled nitrogen sources in the tissue culture media rather than from any transamination from the tracer (Figure 1A). This is not the case for intracellular Mtb. For example, labeled nitrogen from $^{15}N_1$-Asp, $^{15}N_1$-Glu, or $^{15}N_2$-Gln was incorporated predominantly into Asp/n, Glu/n, and isoleucine (Ile) in the macrophage, but labeling was measured in nearly all amino acids derived from intracellular

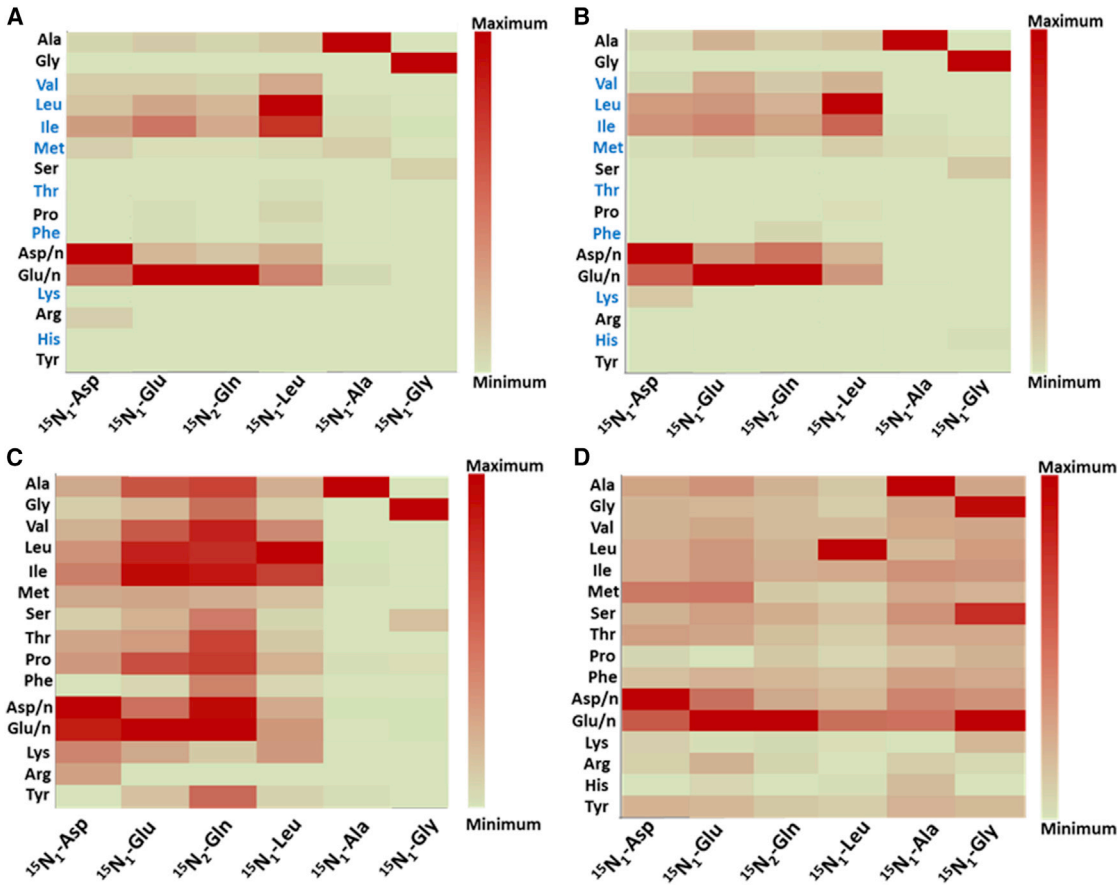

Figure 1. Assimilation Pattern of Different Nitrogen Sources

(A–D) Heatmaps are shown for amino acids derived from Mtb-infected macrophages (A), uninfected macrophages (B), intracellular Mtb (C), and *in-vitro*-grown Mtb in rosins minimal media (D). Assimilation patterns are shown for six tracers: $^{15}N_1$-Asp, $^{15}N_1$-Glu, $^{15}N_2$-Gln, $^{15}N_1$-Leu, $^{15}N_1$-Ala, and $^{15}N_1$ Gly. Essential amino acids for macrophages are highlighted in blue. Heatmaps were produced using enrichment (%) of amino acids recorded for each of the individual tracer experiments in Data S1. The maximum and minimum enrichments for each heatmap are described using color keys. Enrichments are shown for the following amino acids: alanine (Ala), m/z 260; glycine (Gly), m/z 246; valine (Val), m/z 288; leucine (Leu), m/z 274; isoleucine (Ile), m/z 274; methionine (Met), m/z 320; serine (Ser), m/z 390; threonine (Thr), m/z 404; proline (Pro), m/z 258; phenylalanine (Phe), m/z 336; aspartate/asparagine (Asp/n), m/z 418; glutamate/glutamine (Glu/n), m/z 432; lysine (Lys), m/z 431; arginine (Arg), m/z 442; and tyrosine (Tyr), m/z 466, measured using GC-MS.

Mtb (Figures 1A and 1C). These data also reveal potential directions of transamination in Mtb. For example, nitrogen from $^{15}N_2$-Gln was assimilated into six amino acids—Asp/n, Glu/n, Ile, Leu, valine (Val), or Ala in infected macrophages (Figure 1A)—whereas in Mtb, eight additional amino acids were labeled (Figure 1C). As the label from Gln has already been transaminated into several amino acids in the macrophage, any of those macrophage's amino acids could be the source of the Mtb's labeled nitrogen.

Nitrogen Metabolism Is Compartmentalized when Mtb Is Growing Intracellularly

Our results demonstrate that nitrogen was assimilated differently, depending on the original amino acid source in intracellular Mtb. We use the term "compartmentalization" to refer to the selective transfer of nitrogen from the tracers to other amino acids (Figure 1C). For example, nitrogen from $^{15}N_1$-Asp, $^{15}N_1$-Glu, $^{15}N_2$-Gln, and $^{15}N_1$-Leu was incorporated into many additional amino acids, but nitrogen from $^{15}N_1$-Ala and $^{15}N_1$-Gly was incorporated predominantly into only Ala, Gly, and serine (Ser) pools, respectively. The enrichment profiles for amino acids obtained from the tracers were also distinct. For example, more than 50% of ^{15}N from $^{15}N_1$-Asp was transferred to Glu/n: $^{15}N_1$-Glu to six amino acids, $^{15}N_2$-Gln to eight amino acids, and $^{15}N_1$-Leu to Ile (Figures 1C and 2A). Also, some amino acids were preferentially labeled by particular tracers. For example, the labeling of tyrosine (Tyr) indicates that the nitrogen is transferred from $^{15}N_1$-Glu/$^{15}N_2$-Gln but not from $^{15}N_1$-Asp or any other tracers used. Similarly, nitrogen in arginine (Arg) can be donated by $^{15}N_1$-Asp, but not from any other tested amino acid (Figure 1C). To investigate whether the compartmentalized nitrogen distribution is restricted to intracellular growth of Mtb, we performed similar ^{15}N tracer experiments with Mtb grown in Roisin's minimal media, with glycerol and ammonium chloride as the carbon and nitrogen source, respectively, with the addition of ^{15}N labeled tracers.

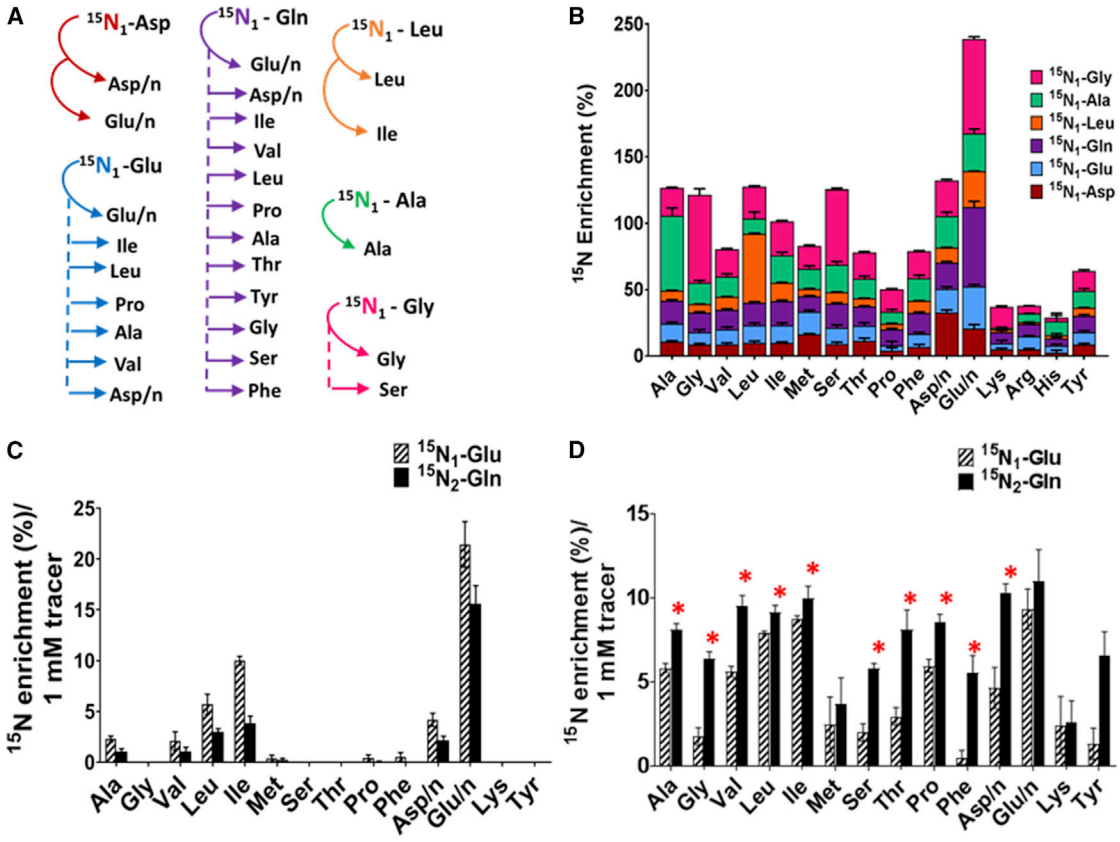

Figure 2. Nitrogen Assimilation is Compartmentalized in Mtb

(A) Distinct enrichment of amino acids from each of the tracers in intracellular Mtb.

(B) ^{15}N assimilation from the tracers into the amino acids in *in-vitro*-grown Mtb.

(C) Comparison of ^{15}N enrichment from the tracers $^{15}N_1$-Glu and $^{15}N_2$-Gln in an infected macrophage.

(D) Comparison of ^{15}N enrichment from the tracers $^{15}N_1$-Glu and $^{15}N_2$-Gln in intracellular Mtb.

Values are mean ± SEM from 3–4 biological replicates. Statistically significant differences were calculated using Holm-Sidak multiple t tests; *$p < 0.001$.

As can be seen, the results demonstrated compartmentalized distribution of ^{15}N from Asp, Glu, Gln, Leu, Ala, and Gly in to the amino acid pools (Figures 2B and S2), extending the finding of Agapova et al. (2019), who demonstrated the compartmentalized distribution of nitrogen from Gln and Asn during *in vitro* growth of Mtb. It is noteworthy that the promiscuous pattern of distribution of nitrogen from both $^{15}N_1$-Ala and $^{15}N_1$-Gly *in vitro* is very different from the restricted distribution found for intracellular Mtb (Figures 1C, 2B, S3E, and S3F). To check whether this promiscuous label distribution in *in-vitro*-grown Mtb was biased by the experimental method, we harvested amino acids from *in-vitro*-grown Mtb using the same method as described for intracellular Mtb. We found no difference in label distribution from $^{15}N_1$-Ala and $^{15}N_1$-Gly in *in-vitro*-grown Mtb using the two methods, which confirmed that the non-promiscuous pattern of these tracers in intracellular Mtb was not experimentally biased (Figure S2, II). The non-promiscuous pattern for these two tracers in intracellular Mtb suggests that these amino acids are scarce, in comparison to other amino acids such as Gln within the Mtb phagosome, and are therefore incorporated directly into biomass by Mtb, rather than being used as nitrogen donors.

Out of all the nitrogen sources tested, nitrogen from $^{15}N_2$-Gln was most widely distributed to other amino acids in intracellular Mtb, suggesting that Gln is the principal nitrogen donor for Mtb during intracellular growth (Figures 1C and 2A). The comparison of enrichment profiles between $^{15}N_1$-Glu and $^{15}N_2$-Gln demonstrated that both tracers gave similar ^{15}N distribution patterns in amino acids derived from an uninfected macrophage and an infected macrophage (Figures 1A and 1B), but $^{15}N_2$-Gln provided significantly higher enrichments than $^{15}N_1$-Glu for the majority of the intracellular Mtb amino acids (Figure 1C). Direct comparison of $^{15}N_1$-Glu and $^{15}N_2$-Gln demonstrated that there were no significant differences in enrichments between $^{15}N_1$-Glu and $^{15}N_2$-Gln in the macrophage (Figure 2C). But in the case of intracellular Mtb, using the tracer $^{15}N_2$-Gln resulted in significant enrichments for the majority of amino acids (Figure 2D).

Uptake versus *De Novo* Synthesis of Amino Acids in Intracellular Mtb

To further evaluate the role of each macrophage amino acid pool in the provision of nitrogen to intracellular Mtb, we calculated the nitrogen incorporation ratio (NIR) between ^{15}N enrichment of amino acids in intracellular Mtb and the same amino acid in

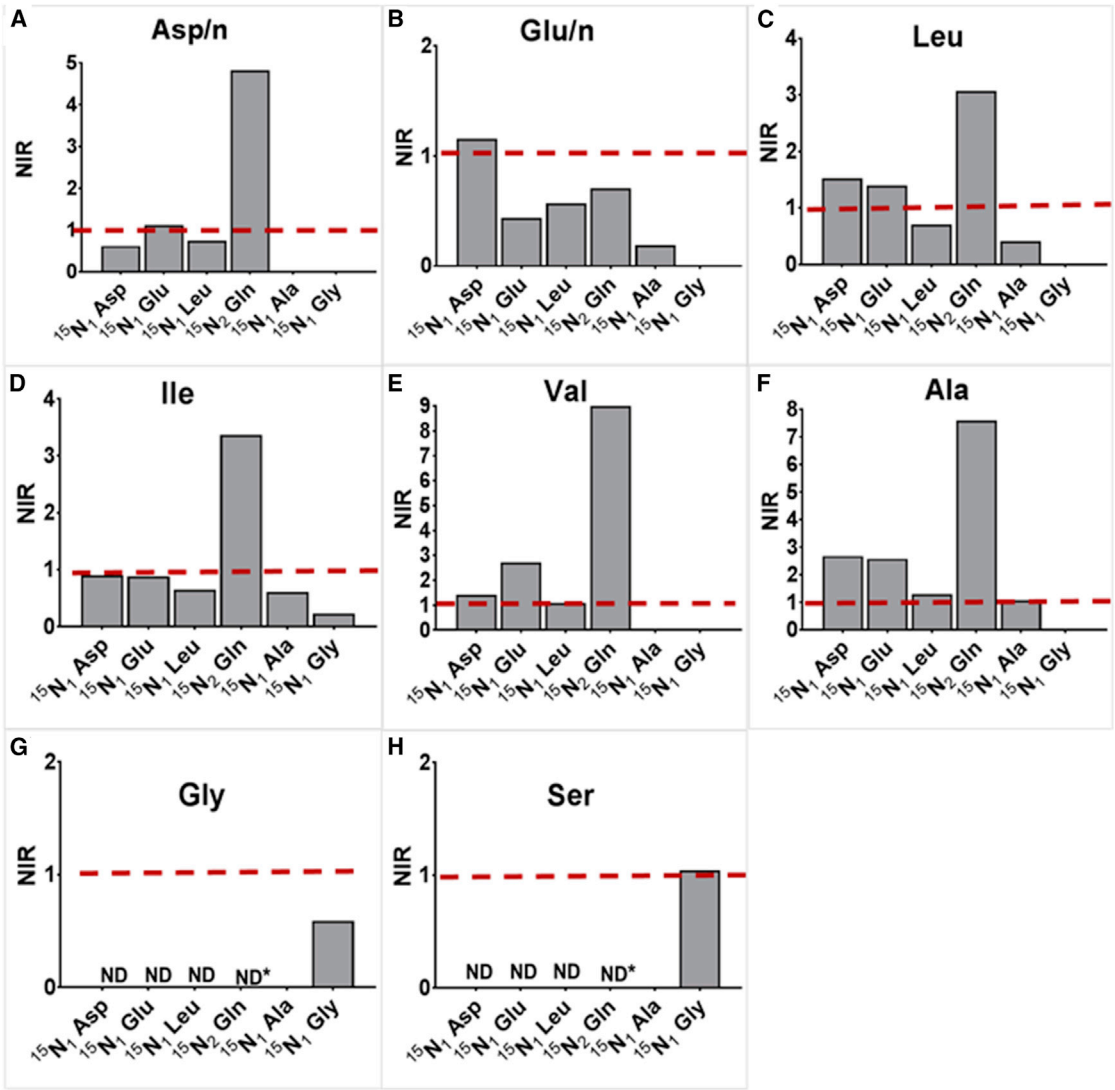

Figure 3. Uptake versus *De Novo* Synthesis of Amino Acids in Intracellular Mtb

(A–H) The NIR of ^{15}N enrichment (%) in intracellular Mtb to infected macrophages is shown for Asp/n, m/z 418 (A), Glu/n, m/z 432 (B), Leu, m/z 274 (C), Ile, m/z 274 (D), Val, m/z 288 (E), Ala, m/z 260 (F), Gly, m/z 246 (G), and Ser, m/z 390 (H). An NIR of 1 indicates that the particular amino acid in Mtb was acquired directly from the macrophage. NIRs were calculated from the enrichments measured from 3–8 individual macrophage infection experiments using the tracers $^{15}N_1$-Asp, $^{15}N_1$-Glu, $^{15}N_2$-Gln, $^{15}N_1$-Leu, $^{15}N_1$-Ala, and $^{15}N_1$-Gly. Ratios that were not determined for Gly (G) and Ser (H) are indicated by ND, and the asterisk indicates maximum ^{15}N detected in Mtb from $^{15}N_2$-Gln.

the host macrophage. Amino acids acquired directly from the host that are not subject to any additional synthesis or metabolism will have similar ^{15}N enrichment as the macrophage amino acids and an NIR of 1. *De novo* synthesis or additional metabolic processes, such as transamination reactions, will be revealed by different levels of ^{15}N enrichment of amino acids in Mtb, compared with that of macrophage amino acids. Figures 3A–3G show the ratio of ^{15}N enrichment for seven amino acids derived from intracellular Mtb compared with amino acids derived from infected macrophages. Amino acids Val, Ile, and Ala had an NIR of 1 for more than one tracer tested as the source of label, suggesting the uptake of these amino acids is directly from the macrophage by Mtb (Figures 3D–3F). Also, the NIR was >1 when $^{15}N_2$-Gln was used as the tracer, suggesting the biosynthesis of these amino acids in addition to the uptake. Further clues as to the level of uptake versus biosynthesis can be gleaned from closer inspection of the data. For example, when $^{15}N_1$-Asp was used as the label for the Asp/n pool, the NIR was <1 (Figure 3A), indicating that any Mtb Asp/n imported from the macrophage was being diluted with nitrogen from a source that was less labeled than the macrophage Asp/n pool. However, when $^{15}N_2$-Gln was used as the tracer, the ratio for the Asp/n pools was >4, indicating that any Mtb Asp/n imported from the macrophage was being diluted with nitrogen from a source that was at least 4× more labeled than Asp/n pools from the macrophage. The same was not true when $^{15}N_1$-Glu

was the source of the label. The obvious conclusion is that the Asp's nitrogen in Mtb is largely derived from the macrophage Gln. Overall, using the tracer $^{15}N_2$-Gln resulted in the highest levels of labeling for the majority of the amino acids analyzed, confirming our previous conclusion that Gln is the predominant nitrogen donor for intracellular Mtb.

NIR analysis also revealed the exclusivity of nitrogen distribution in the Gly and Ser pools of intracellular Mtb (Figures 3G and 3H). Nitrogen from Gly is not promiscuous, as the label from $^{15}N_1$-Gly remained with the Gly and Ser pools. Therefore, Gly is not a nitrogen donor for Mtb. For Gly, a homologous labeling with $^{15}N_1$-Gly gave an NIR less than 1, indicating that Mtb's Gly pool is being diluted by a less labeled nitrogen source, but not any of the tested amino acids, since none of them gave significant levels of incorporation into Gly (Figure 3G). None of the tracers tested provided nitrogen to Ser, except for Gly. The NIR of Ser was 1 for the label from $^{15}N_1$-Gly, indicating the biosynthesis of Ser, in which imported Gly is converted to Ser in intracellular Mtb (Figure 3H).

Development of ^{15}N-FSRA to Probe the Uptake of Nitrogen Sources from the Host by Mtb

Qualitative conclusions about the uptake of nitrogen sources can be drawn from simple labeling patterns generated by $^{15}N_1$-Ala and $^{15}N_1$-Gly (Figures S3, I and II); however, the Figure S3 NIR does not account for the intracellular redistribution of nitrogen. Here, we can use neither the traditional ^{13}C Metabolic Flux Analysis (MFA), since we want to infer the uptake, nor our former ^{13}C-FSA tool, since we have to take too many possible uptakes into account. We therefore developed ^{15}N-FSRA to model the nitrogen source uptake by intracellular Mtb. This approach inputs data from the ^{15}N tracer experiments into an *in silico* model of central nitrogen metabolism in Mtb, but without making a prior assumption on the number or combination of potential nitrogen sources. The method calculates the range of potential explanations in terms of nitrogen uptake flux relative to biomass contribution, which is consistent with the available labeling datasets simultaneously. We call this the flux spectral range (FSR). The FSR of an amino acid gives an unbiased possibilistic measure, reflecting the possible nitrogen flows.

A ^{15}N metabolic model was constructed for Mtb including nitrogen atom transitions and reaction reversibilities (Data S2; Figure S4). The model was able to analyze the amino acid pairs Glu/Gln and Asp/Asn as separate pools and was solely constrained by the biomass equation taken from our previous work (Beste et al., 2011). The uptake of ^{15}N labeled amino acids by Mtb was modeled by using the macrophage-derived amino acid mass isotopomer distributions as potential intracellular nitrogen sources. The measurements of all six tracer experiments were incorporated into the model. From the labeling data measurements, histidine (His), Arg, cysteine (Cys), and tryptophan (Trp) were excluded due to the low levels detected. The relative FSRs (minimum ratio, median, and maximum ratio) of amino acid nitrogen uptake flux to the nitrogen content of each amino acid in biomass were deduced (Data S3). For this analysis, amino acids with minimum/maximum FSR of ~1 indicated that this amino acid is available in the macrophage and fully incorporated into Mtb's biomass, whereas a minimum/maximum FSR of 0 indicates that the amino acid is unavailable and must be completely synthesized *de novo* by Mtb. A minimum or maximum FSR >1 indicates that the uptake of the amino acid is greater than the biomass requirements; therefore, this amino acid is a likely nitrogen donor. It should be noted that amino acids with FSRs between 0 and 1 may still be nitrogen donors, but the deficit in their uptake compared to biomass requirement must be made up by *de novo* synthesis with an alternative nitrogen source.

^{15}N-FSRA identified 14 amino acids (minimum ratio > 0) that are available and taken up by intracellular Mtb from the macrophage (Table 1). Nine amino acids had FSRs between 0 and 1, and the biomass nitrogen requirement was met by *de novo* synthesis. The narrow FSR of 1 for Ala confirmed our previous analysis that this amino acid was taken up by Mtb from the macrophage and incorporated directly into the biomass. The analysis showed that Gln and Val are both used as nitrogen donors for the synthesis of other amino acids with high certainty (minimum FSR > 1). For Asp and Gly, the minimum FSR was >0 and the maximum >1, and they are synthesized *de novo* but could also be taken up by Mtb and used as nitrogen donors. Furthermore, our results revealed that nine amino acids (Asn, Ile, Leu, methionine [Met], Lys, Tyr, phenylalanine [Phe], proline [Pro], and threonine [Thr]) are synthetized *de novo* to suffice biomass requirements for growth in varying proportions, as seen from the narrow ratio ranges. The roles of Ser and Glu as nitrogen donors could not be resolved computationally, as the minimum FSR was 0 (not taken up from the macrophage) and maximum FSR > 1 (taken up in excess).

Serine Biosynthesis Is Essential for the Intracellular Survival of Mtb

^{15}N-FSRA predicted the minimum FSR of Ser to be 0, indicating that there was no uptake of this amino acid from the macrophage and that its biosynthesis is essential for Mtb's survival inside the host. To test this prediction, we constructed a serine auxotroph of Mtb and tested its survival in macropgaes. Ser is biosynthesized in a multistep reaction using 3-phosphoglyceric acid (PGA) as the precursor produced during glycolysis. Phosphoserine transaminase *ser*C (Rv0884c) catalyzes the addition of nitrogen to the carbon backbone of pyruvate to form Ser (Figure 4A; Bai et al., 2011). In addition to being a proteinogenic amino acid, Ser provides the nitrogen backbone for the synthesis of Gly and Cys and also replenishes the pyruvate pool in central carbon metabolism (Figure 4A). Phosphoserine transaminase *ser*C, the enzyme that aminated pyruvate to form Ser, was predicted to be essential for the growth of Mtb *in vitro* (DeJesus et al., 2017). Here, we successfully generated the Δ*serC* H37Rv Mtb strain. The Δ*serC* strain failed to grow without Ser supplementation, compared to the wild-type (WT) and the complemented strain, Δ*serC*::serC (Figure 4B), confirming serine auxotrophy. Unlike other nitrogen sources that were promiscuous when tested in *in vitro* (Figure 1D), Ser was not a widely assimilated *in vitro* nitrogen source; nitrogen from $^{15}N_1$-Ser was distributed predominantly to Gly (Figure 4C). This result demonstrates the distinct nitrogen distribution between Ser and Gly via serine hydroxymethyltransferase *glyA1*, *glyA2* (Figure 4A) and was in concord with our earlier analyses in

Table 1. Flux Spectral Ranges Determined with ^{15}N FSRA

Category	Nitrogen Source	Flux Spectral Range		
		Minimum Ratio	Maximum Ratio	Median
↓	Asn	0.06	0.19	0.13
↓	Pro	0.31	0.38	0.34
↓	Thr	0.37	0.49	0.43
↓	Ile	0.52	0.64	0.55
↓	Tyr	0.57	0.63	0.60
↓	Leu	0.58	0.96	0.61
↓	Met	0.64	0.77	0.68
↓	Phe	0.63	0.75	0.69
↓	Lys	0.78	0.82	0.81
→	Ala	0.98	1	1
0/○	Glu	0	1.63	0.02
0/○	Ser	0	3.59	1.31
○	Gly	0.51	3.17	0.67
○	Asp	0.61	12.46	2.11
↑	Gln	1.50	11.85	2.47
↑	Val	1.82	13.45	2.88

Minimum and maximum FSRs for all computationally accessible amino acids and the median of their distributions (Data S3). Amino acids are grouped into five categories: ↓, spectral ranges in the interval [0,1) indicate that the biomass nitrogen need has to be fulfilled by *de novo* synthesis of the amino acid; →, spectral range is essentially 1, nitrogen biomass requirement is balanced with uptake, and no nitrogen is shared; 0, the amino acid is not taken up; ○, spectral range is inconclusive, as the amino acid might be synthesized *de novo*, but may also be a nitrogen donor; ↑, spectral ranges are larger then 1, indicating that this amino acid is available as a nitrogen donor.

Figures 1C and 3H. Furthermore, Δ*serC* was strongly attenuated for intracellular survival in THP-1 macrophages, as compared with WT H37Rv and the complemented strain (Figures 4D and 4E). These data validate the ^{15}N-FRSA predictions and confirm that serine biosynthesis is essential for the intracellular survival of Mtb.

DISCUSSION

We and others have shown that Mtb co-metabolizes multiple carbon sources during intracellular growth in the human host cell (Beste et al., 2013; Ehrt et al., 2018; McKinney et al., 2000). Here, we demonstrate that this is also the case for nitrogen. Using ^{15}N isotopomer profiling and ^{15}N-FSRA systems-based inference tool, we describe the first nitrogen metabolic phenotype of Mtb inside human macrophages (Figure 5). With the ^{15}N-FSRA tool, we predicted that Mtb has access to most amino acids within the macrophage (Table 1), and this uptake was insufficient to meet the biomass requirement for most tested amino acids and therefore must be complemented with *de novo* synthesis from nitrogen donors. This analysis identified the amino acids Asp, Glu, Gln, Val, Leu, Ala, and Gly as the intracellular nitrogen sources utilized by Mtb in human macrophages.

Further analysis of the data demonstrated that, like carbon metabolism in Mtb (de Carvalho et al., 2010), nitrogen metabolism is compartmentalized (Figures 1C and 1D). Our *in vitro* results (Figure 1D) are consistent with the results of Agapova et al. (2019), who demonstrated that Mtb does not show a preference for any amino acids as nitrogen sources when grown *in vitro*. However, in this study, we demonstrate that this is clearly not the case for Mtb growing inside macrophages. Instead, the principal nitrogen source for intracellular Mtb appears to be Gln, but there is a clear pattern of compartmentalization of distribution of nitrogen with some sources: Gln is a highly promiscuous nitrogen donor, whereas other amino acids, such as Gly and Ala, have a restrictive pattern of nitrogen distribution. Metabolism has been shown to be compartmentalized in other bacteria with microcompartments, such as carboxysomes and metabolosomes, serving to compartmentalize enzymes involved in particular pathways and to restrict the exposure of toxic intermediates to the rest of the cell (Frank et al., 2013). For example, in *Salmonella enterica*, activity of the metabolosome was required to alleviate acetaldehyde toxicity during ethanolamine catabolism (Brinsmade et al., 2005). In the case of intracellular Mtb, different nitrogen sources might be assimilated using enzymes that are similarly localized. For example, enzymes glutamine synthetase and asparaginase are demonstrated to function extracellularly for the catabolism of Gln and Asn, respectively, in Mtb (Harth et al., 1994; Gouzy et al., 2014a) as a strategy to resist acidic stress inside the phagosome.

Earlier studies demonstrated that Asp is an intracellular nitrogen source for Mtb, and the pathways for Asp/n assimilation were recently described (Gouzy et al., 2013, 2014a). However, although our results confirm that Asp is indeed a nitrogen source, they also demonstrate that, of the tested amino acids, Gln is the principal source of nitrogen for intracellular Mtb and is the amino acid whose nitrogen is most widely assimilated (Figure 1C). Gln is the major fuel for a variety of mammalian cells including macrophages (Zhang et al., 2017), and THP-1 macrophages have previously been shown to assimilate Gln into Glu (Amorim Franco et al., 2017; Zhao et al., 2013; Choi and Park, 2018). Our previous study demonstrated that carbon from both Glu and Gln was available to Mtb inside the macrophage (Beste et al., 2013). Here, we additionally show that Gln, and not Glu, is the predominant nitrogen donor for intracellular Mtb. Once in Mtb, Gln can be converted to Glu by glutamate synthase (GltB) (Lee et al., 2018), and the nitrogen is transferred to other amino acids by various transaminases (Figure 5). Our results are thereby consistent with previous studies that have demonstrated that Glu/n biosynthesis is essential for the intracellular growth and survival of Mtb (Harper et al., 2008; Gallant et al., 2016; Ventura et al., 2013; Tullius et al., 2003). In addition to being the nitrogen donor for other amino acids, Glu/n is also involved in cell wall synthesis and resisting acid and nitrosative stress (Harth and Horwitz, 2003; Wietzerbin-Falszpan et al., 1973; Read et al., 2007). These studies, together with our results, establish Glu/n as the hub of nitrogen metabolism in intracellular Mtb. Gln was involved in modulating host cellular immune responses (Dos Santos et al., 2017), and Mtb infection increased macrophage's metabolic dependency on Gln (Cumming et al., 2018). We found no significant changes in macrophage's $^{15}N_2$-Gln assimilation profile upon infection by Mtb (Figure 1A), but there could be an increase in the pool sizes of Gln and its related pathway

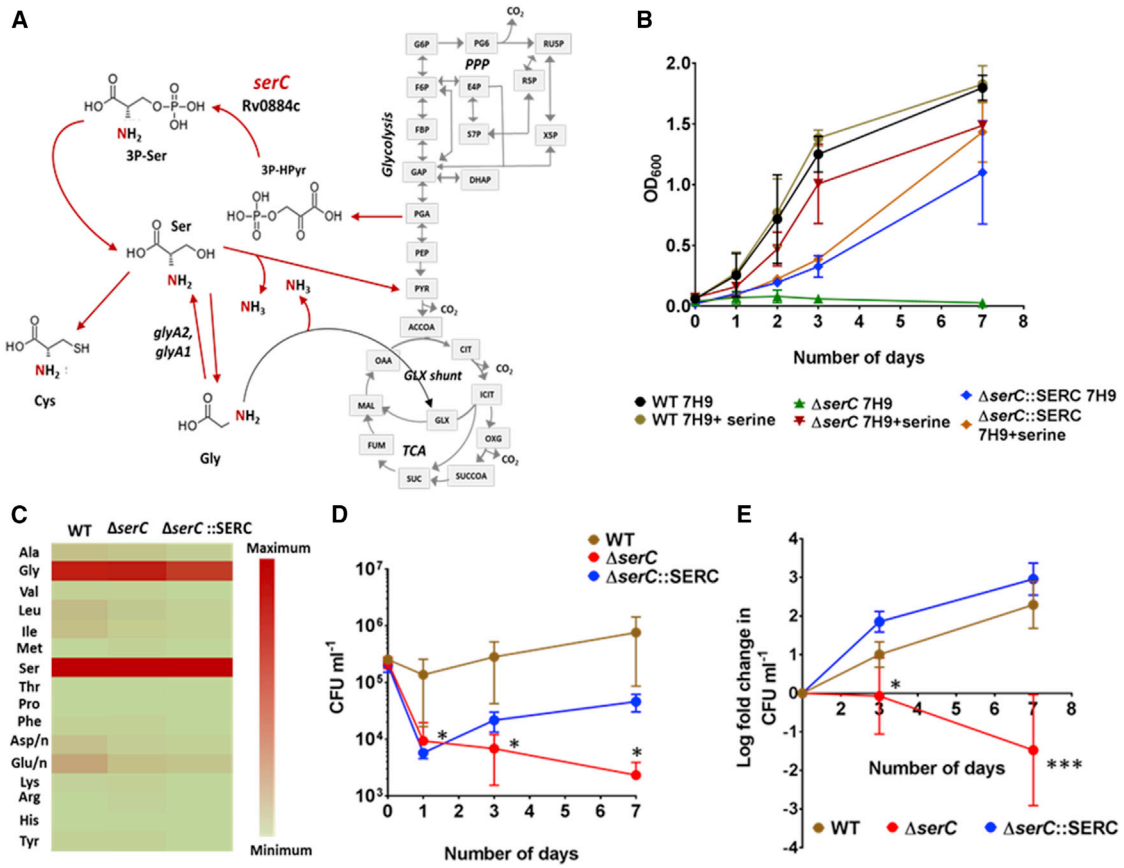

Figure 4. Serine Biosynthesis Is Essential for the Intracellular Survival of Mtb

(A) Metabolic role of *serC* in Mtb. *serC* catalyzes the production of serine from pyruvate. Gly, Cys, and pyruvate are synthesized from Ser.

(B) Growth of wild-type (WT), Δ*serC* mutant, and complement Δ*serC*::SERC in 7H9 medium supplemented with 10% oleic acid, albumin, dextrose, and catalase (OADC) tested with and without the addition of Ser. Data are the average of three biological replicates ± SD.

(C) Assimilation of $^{15}N_1$-SER by WT, Δ*serC*, and Δ*serC*::SERC in Rosin's minimal medium with glycerol and NH_4Cl. Data are the average of three biological replicates ± SD.

(D) Growth of WT, Δ*serC*, and Δ*serC*::SERC in THP-1 macrophages. CFUs (colony forming units) of the three strains were recorded for 0 (before infection), 1, 3, and 7 days post-infection.

(E) Fold change in CFUs of the three strains over the period of infection.

Data are the average of six independent infection experiments, each with three technical replicates for WT and Δ*serC* and one for infection with four technical replicates for Δ*serC*::SERC ± SD. Statistically significant reduction in CFU counts and fold change in CFUs for Δ*serC* as compared to the WT and complement was calculated using Student's t test. *$p < 0.05$; ***$p < 0.0005$. PPP, pentose phosphate pathway; TCA, tricarboxylic acid cycle; 3P-HPyr, 3-phosphonooxypyruvate; 3P-Ser, 3-Phosphoserine; Cys, cysteine; PGA, 3-phosphoglyceric acid; PYR, pyruvate; PEP, phosphoenolpyruvate; GAP, glyceraldehyde 3phosphate; DHAP, dihydroxyacetone phosphate; G6P, glucose-6-phosphate; F6P, fructose 6-phosphate; FBP, fructose bisphosphate; PG6, phosphogluconolactone; RU5P, riboluse 5-phosphate; R5P, ribose 5-phosphate; E4P, erythrose 4-phosphate; S7P, sedoheptoluse 7-phsophate; X5P, xylulose 5-phosphate; ACCCOA, AcetylCoA; OAA, oxaloacetic acid; MAL, malate; FUM, fumarate; SUC, succinate; SUCCOA, succinyl CoA; OXG, 2-oxoglutarate; ICIT, isocitrate; CIT, citrate.

intermediates. This leads to an intriguing hypothesis that Mtb may facilitate its own intracellular survival by metabolizing Gln in the host, and targeting Glu/n transport and metabolism therefore represents a promising avenue for the development of anti-TB drugs.

Biosynthesis of branched chain amino acids is also essential for the intracellular survival of Mtb (Awasthy et al., 2009). Here, we show that the branched chain amino acid Val is acquired directly by intracellular Mtb and is utilized as a nitrogen donor in addition to Gln (Figure 3; Table 1). Val was not directly tested as a tracer for the ^{15}N experiments in the macrophage and intracellular Mtb, but the Val pool was ^{15}N labeled from all of the amino acid tracers (except for $^{15}N_1$-Ala and $^{15}N_1$-Gly), suggesting that nitrogen was shared between Val and other amino acids. A Val auxotroph of Mtb was able to survive in macrophages (Awasthy et al., 2009); this is consistent with our FSRA predictions that intracellular Mtb acquired Val from the host. Nitrogen from Val is reversibly transaminated to Glu, Ile, and Leu by *ilvE*, the branched chain transaminase that is required for mycobacterial survival during infection in the mice model (Grandoni et al., 1998; Sassetti and Rubin, 2003; Tremblay and Blanchard, 2009). The demonstration by

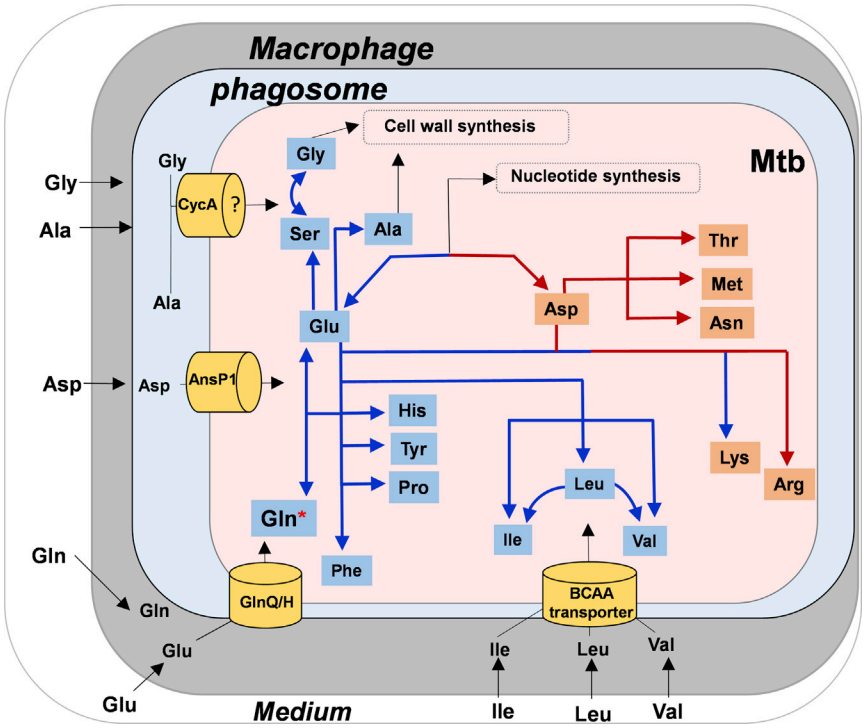

Figure 5. Schematic Representation of Nitrogen Metabolism (Acquisition and Assimilation) in Intracellular Mtb

Macrophages acquires nitrogen sources Asp (aspartate), Glu (glutamate), Gln (glutamine), Leu (leucine), Ala (alanine), and Gly (glycine) directly from the growth media. Glu/Gln is taken from the host via yet-unidentified transporter. Asp is accessible to intraphagosomal Mtb, which it uptakes from the host macrophages via AnsP1 (Gouzy et al., 2014a). Leu, Ile (isoleucine), and Val (valine) are acquired from the host macrophages via yet-unindentified branched chain amino acid, probably an ABC-type transporter. Ala, Gly, and Ser are possibly acquired via CycA transport system. Gln, Val, and Asp were potential nitrogen donors for cellular protein synthesis, with Gln as the principal nitrogen donor in intracellular Mtb (indicated by asterisk). Nitrogen from Gln was transaminated primarily to Glu and Asp for the synthesis of other amino acids. Ala and Gly are assimilated mainly into Ala, Gly, and Ser pools. Limited transamination of nitrogen from Ala and Gly to other amino acids suggests direct assimilation of these two amino acids for biomass-cell wall synthesis.

Zimmermann et al. (2017) that the biosynthetic genes for branched chain amino acids were downregulated when Mtb was growing intracellularly in macrophages is consistent with our evidence that these amino acids are also available in the phagosome. Our finding that nitrogen from Leu is assimilated by intracellular Mtb is surprising, since a Δ*leuD* auxotroph of Mtb was shown to be severely attenuated for growth and virulence in murine bone-marrow-derived macrophages and in mice, suggesting that Leu was unavailable to Mtb growing within its host (Chen et al., 2012; Hondalus et al., 2000; Sampson et al., 2004). The ^{15}N-FSRA showed that Leu uptake is insufficient for Mtb's biomass requirements, indicating that the uptake must be supplemented by *de novo* synthesis, consistent with the auxotrophic results.

Our previous work showed that the carbon backbone of Ala was acquired from the host and directly incorporated into Mtb's biomass (Beste et al., 2013). Here, we show that Ala was not a nitrogen donor for intracellular Mtb (Figure 1C; Table 1). Gly was also a nitrogen source for intracellular Mtb, but its nitrogen was similarly not widely assimilated. Both Ala and Gly are components of the mycobacterial cell wall (Alderwick et al., 2015; Mahapatra et al., 2005; Wietzerbin-Falszpan et al., 1973), so it seems likely that these amino acids acquired from the host are directly incorporated into cell wall synthesis (Beste et al., 2013). ^{15}N-FSRA predicted zero uptake of Ser, suggesting that its biosynthesis may be essential for the intracellular replication of Mtb and thereby a potential drug target. To test this hypothesis, we constructed a Ser auxotroph of Mtb and demonstrated that it is severely attenuated for growth in the macrophage. Our findings validate our systems-based approach and highlight Ser biosynthesis, and particularly the transaminase *serC*, as a potential drug target.

In addition to biosynthesis, the transport systems of nitrogen sources are potential targets for anti-TB drug development. However, there is only limited knowledge of the amino acid transport systems in Mtb (Cook et al., 2009). The Asp transporter AnsP1 is essential for the virulence of Mtb in murine models (Gouzy et al., 2013). Although Glu and branched chain amino transport systems are yet to be identified, the *Streptococcus mutans* and *Lactococcus lactis glnQHMP* system is known to transport Glu (Krastel et al., 2010; Fulyani et al., 2015), and Mtb encodes GlnQ and GlnP homologs that could function as Glu/n transporters (Cole et al., 1998; Braibant et al., 2000). The common transporter for Ala, Gly, and Ser, cycA, also remains unstudied (Awasthy et al., 2012; Chen et al., 2012; Cole et al., 1998). Further investigations are required to define these amino acid transporters of Mtb.

In summary, we describe the first nitrogen metabolic phenotype of intracellular Mtb and the development and application of a novel computational systems-based tool, ^{15}N-FSRA, to investigate nitrogen uptake and assimilation of not only Mtb, but also any intracellular pathogen, in complement with direct isotopic labeling interpretation. In conclusion, we have identified that multiple nitrogen sources are acquired and assimilated by Mtb inside the host macrophages, and Gln is the principal intracellular nitrogen donor. The biosynthetic and transport systems of these identified nitrogen sources—and in particular, phosphoserine transaminase—involved in Ser biosynthesis are a target for the development of innovative anti-TB therapies.

STAR★METHODS

Detailed methods are provided in the online version of this paper and include the following:

- KEY RESOURCES TABLE
- LEAD CONTACT AND MATERIALS AVAILABILITY
- EXPERIMENTAL MODEL AND SUBJECT DETAILS
- METHOD DETAILS
  - Mycobacterium tuberculosis (Mtb) cultivation
  - THP-1 macrophage cultivation
  - ^{15}N isotopic labeling during infection of macrophages with Mtb
  - *In vitro* ^{15}N isotopic labeling
  - Gas-chromatography mass spectrometry (GC-MS) and ^{15}N mass isotopomer analysis
  - Nitrogen network model (of Mtb)
  - ^{15}N Flux Spectral Range Analysis (^{15}N-FSRA)
  - Construction of serC (Rv0884c) knockout strain of H37Rv
  - Construction of the complement strain ΔserC::SERC H37Rv
  - Growth of ΔserC and ΔserC::SERC H37Rv strains
  - Macrophage infections with WT, ΔserC and ΔserC::SERC H37Rv strains
  - $^{15}N_1$-serine isotopic labeling
- QUANTIFICATION AND STATISTICAL ANALYSIS
- DATA AND CODE AVAILABILITY

SUPPLEMENTAL INFORMATION

Supplemental Information can be found online at https://doi.org/10.1016/j.celrep.2019.11.037.

ACKNOWLEDGMENTS

This study was supported by the Biotechnology and Biological Sciences Research Council (BBSRC) grant (BB/L022869/1) and Medical Research Council (MR/K01224X/1), United Kingdom.

AUTHOR CONTRIBUTIONS

Conceptualization, K.B., D.J.V.B., K.N., and J.M.; Methodology, K.B., D.J.V.B., J.M., and K.N.; Investigation, K.B., M.B., and T.A.M.; Writing – Original Draft, K.B., D.J.V.B., and J.M.; Writing – Review and Editing, K.B., H.W., P.B., T.A.M., M.B., K.N., D.J.V.B., and J.M.; Funding Acquisition, D.J.V.B. and J.M.; Resources, J.M.; Supervision, K.N., D.J.V.B. and J.M.

DECLARATION OF INTERESTS

The authors declare no competing interests.

Received: February 18, 2019
Revised: July 5, 2019
Accepted: November 7, 2019
Published: December 10, 2019

REFERENCES

Agapova, A., Serafini, A., Petridis, M., Hunt, D.M., Garza-Garcia, A., Sohaskey, C.D., and de Carvalho, L.P.S. (2019). Flexible nitrogen utilisation by the metabolic generalist pathogen *Mycobacterium tuberculosis*. eLife *8*, e41129.

Alderwick, L.J., Harrison, J., Lloyd, G.S., and Birch, H.L. (2015). The Mycobacterial Cell Wall–Peptidoglycan and Arabinogalactan. Cold Spring Harb. Perspect. Med. *5*, a021113.

Amorim Franco, T.M., Favrot, L., Vergnolle, O., and Blanchard, J.S. (2017). Mechanism-Based Inhibition of the *Mycobacterium tuberculosis* branched-chain aminotransferase by d- and l-cycloserine. ACS Chem. Biol. *12*, 1235–1244.

Awasthy, D., Gaonkar, S., Shandil, R.K., Yadav, R., Bharath, S., Marcel, N., Subbulakshmi, V., and Sharma, U. (2009). Inactivation of the *ilvB1* gene in *Mycobacterium tuberculosis* leads to branched-chain amino acid auxotrophy and attenuation of virulence in mice. Microbiology *155*, 2978–2987.

Awasthy, D., Bharath, S., Subbulakshmi, V., and Sharma, U. (2012). Alanine racemase mutants of Mycobacterium tuberculosis require D-alanine for growth and are defective for survival in macrophages and mice. Microbiology *158*, 319–327.

Bai, G., Schaak, D.D., Smith, E.A., and McDonough, K.A. (2011). Dysregulation of serine biosynthesis contributes to the growth defect of a *Mycobacterium tuberculosis* crp mutant. Mol. Microbiol. *82*, 180–198.

Bardarov, S., Bardarov, S., Jr., Pavelka, M.S., Jr., Sambandamurthy, V., Larsen, M., Tufariello, J., Chan, J., Hatfull, G., and Jacobs, W.R., Jr. (2002). Specialized transduction: an efficient method for generating marked and unmarked targeted gene disruptions in *Mycobacterium tuberculosis, M. bovis* BCG and *M. smegmatis*. Microbiology *148*, 3007–3017.

Beste, D.J., Bonde, B., Hawkins, N., Ward, J.L., Beale, M.H., Noack, S., Nöh, K., Kruger, N.J., Ratcliffe, R.G., and McFadden, J. (2011). ^{13}C metabolic flux analysis identifies an unusual route for pyruvate dissimilation in mycobacteria which requires isocitrate lyase and carbon dioxide fixation. PLoS Pathog. *7*, e1002091.

Beste, D.J., Nöh, K., Niedenführ, S., Mendum, T.A., Hawkins, N.D., Ward, J.L., Beale, M.H., Wiechert, W., and McFadden, J. (2013). ^{13}C-flux spectral analysis of host-pathogen metabolism reveals a mixed diet for intracellular *Mycobacterium tuberculosis*. Chem. Biol. *20*, 1012–1021.

Beyß, M., Azzouzi, S., Weitzel, M., Wiechert, W., and Nöh, K. (2019). The design of fluxml: a universal modeling language for ^{13}C metabolic flux analysis. Front. Microbiol. *10*, 1022.

Braibant, M., Gilot, P., and Content, J. (2000). The ATP binding cassette (ABC) transport systems of Mycobacterium tuberculosis. FEMS Microbiol. Rev. *24*, 449–467.

Brinsmade, S.R., Paldon, T., and Escalante-Semerena, J.C. (2005). Minimal functions and physiological conditions required for growth of salmonella enterica on ethanolamine in the absence of the metabolosome. J. Bacteriol. *187*, 8039–8046.

Buescher, J.M., Antoniewicz, M.R., Boros, L.G., Burgess, S.C., Brunengraber, H., Clish, C.B., DeBerardinis, R.J., Feron, O., Frezza, C., Ghesquiere, B., et al. (2015). A roadmap for interpreting $^{(13)}C$ metabolite labeling patterns from cells. Curr. Opin. Biotechnol. *34*, 189–201.

Chen, J.M., Uplekar, S., Gordon, S.V., and Cole, S.T. (2012). A point mutation in *cycA* partially contributes to the D-cycloserine resistance trait of *Mycobacterium bovis* BCG vaccine strains. PLoS ONE *7*, e43467.

Choi, Y.K., and Park, K.G. (2018). Targeting glutamine metabolism for cancer treatment. Biomol. Ther. (Seoul) *26*, 19–28.

Cole, S.T., Brosch, R., Parkhill, J., Garnier, T., Churcher, C., Harris, D., Gordon, S.V., Eiglmeier, K., Gas, S., Barry, C.E., 3rd., et al. (1998). Deciphering the biology of *Mycobacterium tuberculosis* from the complete genome sequence. Nature *393*, 537–544.

Cook, G.M., Berney, M., Gebhard, S., Heinemann, M., Cox, R.A., Danilchanka, O., and Niederweis, M. (2009). Physiology of mycobacteria. Adv. Microb. Physiol. *55*, 81–182, 318–319.

Cowley, S., Ko, M., Pick, N., Chow, R., Downing, K.J., Gordhan, B.G., Betts, J.C., Mizrahi, V., Smith, D.A., Stokes, R.W., and Av-Gay, Y. (2004). The *Mycobacterium tuberculosis* protein serine/threonine kinase PknG is linked to cellular glutamate/glutamine levels and is important for growth *in vivo*. Mol. Microbiol. *52*, 1691–1702.

Cumming, B.M., Addicott, K.W., Adamson, J.H., and Steyn, A.J. (2018). Mycobacterium tuberculosis induces decelerated bioenergetic metabolism in human macrophages. eLife *7*, e39169. https://doi.org/10.7554/eLife.39169.

Das, P., Lahiri, A., Lahiri, A., Sen, M., Iyer, N., Kapoor, N., Balaji, K.N., and Chakravortty, D. (2010). Cationic amino acid transporters and *Salmonella* Typhimurium ArgT collectively regulate arginine availability towards intracellular *Salmonella* growth. PLoS ONE *5*, e15466.

de Carvalho, L.P., Fischer, S.M., Marrero, J., Nathan, C., Ehrt, S., and Rhee, K.Y. (2010). Metabolomics of *Mycobacterium tuberculosis* reveals compartmentalized co-catabolism of carbon substrates. Chem. Biol. *17*, 1122–1131.

DeJesus, M.A., Gerrick, E.R., Xu, W., Park, S.W., Long, J.E., Boutte, C.C., Rubin, E.J., Schnappinger, D., Ehrt, S., Fortune, S.M., et al. (2017). Comprehensive Essentiality Analysis of the *Mycobacterium tuberculosis* Genome via Saturating Transposon Mutagenesis. MBio *8*, e02133-16.

Dos Santos, G.G., Hastreiter, A.A., Sartori, T., Borelli, P., and Fock, R.A. (2017). L-Glutamine *in vitro* Modulates some Immunomodulatory Properties of Bone Marrow Mesenchymal Stem Cells. Stem Cell Rev. Rep. *13*, 482–490.

Ehrt, S., and Rhee, K. (2013). *Mycobacterium tuberculosis* metabolism and host interaction: mysteries and paradoxes. Curr. Top. Microbiol. Immunol. *374*, 163–188.

Ehrt, S., Schnappinger, D., and Rhee, K.Y. (2018). Metabolic principles of persistence and pathogenicity in *Mycobacterium tuberculosis*. Nat. Rev. Microbiol. *16*, 496–507.

Eylert, E., Herrmann, V., Jules, M., Gillmaier, N., Lautner, M., Buchrieser, C., Eisenreich, W., and Heuner, K. (2010). Isotopologue profiling of Legionella pneumophila: role of serine and glucose as carbon substrates. J. Biol. Chem. *285*, 22232–22243. https://doi.org/10.1074/jbc.M110.128678.

Eisenreich, W., Dandekar, T., Heesemann, J., and Goebel, W. (2010). Carbon metabolism of intracellular bacterial pathogens and possible links to virulence. Nat. Rev. Microbiol. *8*, 401–412.

Eoh, H., Wang, Z., Layre, E., Rath, P., Morris, R., Branch Moody, D., and Rhee, K.Y. (2017). Metabolic anticipation in *Mycobacterium tuberculosis*. Nat. Microbiol. *2*, 17084.

Eylert, E., Schär, J., Mertins, S., Stoll, R., Bacher, A., Goebel, W., and Eisenreich, W. (2008). Carbon metabolism of *Listeria monocytogenes* growing inside macrophages. Mol. Microbiol. *69*, 1008–1017.

Flynn, J.L. (2006). Lessons from experimental *Mycobacterium tuberculosis* infections. Microbes Infect. *8*, 1179–1188.

Frank, S., Lawrence, A.D., Prentice, M.B., and Warren, M.J. (2013). Bacterial microcompartments moving into a synthetic biological world. J. Biotechnol. *163*, 273–279.

Fulyani, F., Schuurman-Wolters, G.K., Slotboom, D.J., and Poolman, B. (2015). Relative rates of amino acid import via the ABC transporter GlnPQ determine the growth performance of *Lactococcus lactis*. J. Bacteriol. *198*, 477–485.

Gallant, J.L., Viljoen, A.J., van Helden, P.D., and Wiid, I.J. (2016). Glutamate dehydrogenase is required by *Mycobacterium bovis* BCG for resistance to cellular Stress. PLoS ONE *11*, e0147706.

Gouzy, A., Larrouy-Maumus, G., Wu, T.D., Peixoto, A., Levillain, F., Lugo-Villarino, G., Guerquin-Kern, J.L., de Carvalho, L.P., Poquet, Y., and Neyrolles, O. (2013). *Mycobacterium tuberculosis* nitrogen assimilation and host colonization require aspartate. Nat. Chem. Biol. *9*, 674–676.

Gouzy, A., Larrouy-Maumus, G., Bottai, D., Levillain, F., Dumas, A., Wallach, J.B., Caire-Brandli, I., de Chastellier, C., Wu, T.D., Poincloux, R., et al. (2014a). *Mycobacterium tuberculosis* exploits asparagine to assimilate nitrogen and resist acid stress during infection. PLoS Pathog. *10*, e1003928.

Gouzy, A., Poquet, Y., and Neyrolles, O. (2014b). Amino acid capture and utilization within the *Mycobacterium tuberculosis* phagosome. Future Microbiol. *9*, 631–637.

Gouzy, A., Poquet, Y., and Neyrolles, O. (2014c). Nitrogen metabolism in *Mycobacterium tuberculosis* physiology and virulence. Nat. Rev. Microbiol. *12*, 729–737.

Grandoni, J.A., Marta, P.T., and Schloss, J.V. (1998). Inhibitors of branched-chain amino acid biosynthesis as potential antituberculosis agents. J. Antimicrob. Chemother. *42*, 475–482.

Harper, C., Hayward, D., Wiid, I., and van Helden, P. (2008). Regulation of nitrogen metabolism in *Mycobacterium tuberculosis*: a comparison with mechanisms in *Corynebacterium glutamicum* and *Streptomyces coelicolor*. IUBMB Life *60*, 643–650.

Harth, G., and Horwitz, M.A. (2003). Inhibition of *Mycobacterium tuberculosis* glutamine synthetase as a novel antibiotic strategy against tuberculosis: demonstration of efficacy *in vivo*. Infect. Immun. *71*, 456–464.

Harth, G., Clemens, D.L., and Horwitz, M.A. (1994). Glutamine synthetase of *Mycobacterium tuberculosis*: extracellular release and characterization of its enzymatic activity. Proc. Natl. Acad. Sci. USA *91*, 9342–9346.

Hondalus, M.K., Bardarov, S., Russell, R., Chan, J., Jacobs, W.R., Jr., and Bloom, B.R. (2000). Attenuation of and protection induced by a leucine auxotroph of *Mycobacterium tuberculosis*. Infect. Immun. *68*, 2888–2898.

Kloosterman, T.G., and Kuipers, O.P. (2011). Regulation of arginine acquisition and virulence gene expression in the human pathogen *Streptococcus pneumoniae* by transcription regulators ArgR1 and AhrC. J. Biol. Chem. *286*, 44594–44605.

Krastel, K., Senadheera, D.B., Mair, R., Downey, J.S., Goodman, S.D., and Cvitkovitch, D.G. (2010). Characterization of a glutamate transporter operon, glnQHMP, in *Streptococcus mutans* and its role in acid tolerance. J. Bacteriol. *192*, 984–993.

Lee, S., Jeon, B.Y., Bardarov, S., Chen, M., Morris, S.L., and Jacobs, W.R., Jr. (2006). Protection elicited by two glutamine auxotrophs of *Mycobacterium tuberculosis and in vivo* growth phenotypes of the four unique glutamine synthetase mutants in a murine model. Infect. Immun. *74*, 6491–6495.

Lee, J.J., Lim, J., Gao, S., Lawson, C.P., Odell, M., Raheem, S., Woo, J., Kang, S.H., Kang, S.S., Jeon, B.Y., and Eoh, H. (2018). Glutamate mediated metabolic neutralization mitigates propionate toxicity in intracellular *Mycobacterium tuberculosis*. Sci. Rep. *8*, 8506.

Leighty, R.W., and Antoniewicz, M.R. (2013). COMPLETE-MFA: complementary parallel labeling experiments technique for metabolic flux analysis. Metab. Eng. *20*, 49–55.

Lin, W., Mathys, V., Ang, E.L.Y., Koh, V.H.Q., Martínez Gómez, J.M., Ang, M.L.T., Zainul Rahim, S.Z., Tan, M.P., Pethe, K., and Alonso, S. (2012). Urease activity represents an alternative pathway for *Mycobacterium tuberculosis* nitrogen metabolism. Infect. Immun. *80*, 2771–2779.

Lofthouse, E.K., Wheeler, P.R., Beste, D.J.V., Khatri, B.L., Wu, H., Mendum, T.A., Kierzek, A.M., and McFadden, J. (2013). Systems-based approaches to probing metabolic variation within the *Mycobacterium tuberculosis* complex. PLoS ONE *8*, e75913.

Lommen, A. (2009). MetAlign: interface-driven, versatile metabolomics tool for hyphenated full-scan mass spectrometry data preprocessing. Anal. Chem. *81*, 3079–3086.

Mahapatra, S., Scherman, H., Brennan, P.J., and Crick, D.C. (2005). N Glycolylation of the nucleotide precursors of peptidoglycan biosynthesis of Mycobacterium spp. is altered by drug treatment. J. Bacteriol. *187*, 2341–2347.

Masakapalli, S.K., Kruger, N.J., and Ratcliffe, R.G. (2013). The metabolic flux phenotype of heterotrophic Arabidopsis cells reveals a complex response to changes in nitrogen supply. Plant J. *74*, 569–582.

McAdam, R.A., Weisbrod, T.R., Martin, J., Scuderi, J.D., Brown, A.M., Cirillo, J.D., Bloom, B.R., and Jacobs, W.R., Jr. (1995). *In vivo* growth characteristics of leucine and methionine auxotrophic mutants of *Mycobacterium bovis* BCG generated by transposon mutagenesis. Infect. Immun. *63*, 1004–1012.

McKinney, J.D., Höner zu Bentrup, K., Muñoz-Elías, E.J., Miczak, A., Chen, B., Chan, W.T., Swenson, D., Sacchettini, J.C., Jacobs, W.R., Jr., and Russell, D.G. (2000). Persistence of *Mycobacterium tuberculosis* in macrophages and mice requires the glyoxylate shunt enzyme isocitrate lyase. Nature *406*, 735–738.

Niederweis, M. (2008). Nutrient acquisition by mycobacteria. Microbiology *154*, 679–692.

Read, R., Pashley, C.A., Smith, D., and Parish, T. (2007). The role of GlnD in ammonia assimilation in *Mycobacterium tuberculosis*. Tuberculosis (Edinb.) *87*, 384–390.

Rossi, M.T., Kalde, M., Srisakvarakul, C., Kruger, N.J., and Ratcliffe, R.G. (2017). Cell-type specific metabolic flux analysis:a challenge for metabolic phenotyping and a potential solution in plants. Metabolites *7*, E59.

Russell, D.G. (2001). *Mycobacterium tuberculosis*: here today, and here tomorrow. Nat. Rev. Mol. Cell Biol. *2*, 569–577.

Rustad, T.R., Sherrid, A.M., Minch, K.J., and Sherman, D.R. (2009). Hypoxia: a window into *Mycobacterium tuberculosis* latency. Cell. Microbiol. *11*, 1151–1159.

Sampson, S.L., Dascher, C.C., Sambandamurthy, V.K., Russell, R.G., Jacobs, W.R., Jr., Bloom, B.R., and Hondalus, M.K. (2004). Protection elicited by a double leucine and pantothenate auxotroph of *Mycobacterium tuberculosis* in guinea pigs. Infect. Immun. *72*, 3031–3037.

Sassetti, C.M., and Rubin, E.J. (2003). Genetic requirements for mycobacterial survival during infection. Proc. Natl. Acad. Sci. USA *100*, 12989–12994.

Schnappinger, D., Ehrt, S., Voskuil, M.I., Liu, Y., Mangan, J.A., Monahan, I.M., Dolganov, G., Efron, B., Butcher, P.D., Nathan, C., and Schoolnik, G.K. (2003). Transcriptional adaptation of *Mycobacterium tuberculosis* within macrophages: insights into the phagosomal environment. J. Exp. Med. *198*, 693–704.

Smith, D.A., Parish, T., Stoker, N.G., and Bancroft, G.J. (2001). Characterization of auxotrophic mutants of *Mycobacterium tuberculosis* and their potential as vaccine candidates. Infect. Immun. *69*, 1142–1150.

Stover, C.K., de la Cruz, V.F., Fuerst, T.R., Burlein, J.E., Benson, L.A., Bennett, L.T., Bansal, G.P., Young, J.F., Lee, M.H., Hatfull, G.F., et al. (1991). New use of BCG for recombinant vaccines. Nature *351*, 456–460.

Tremblay, L.W., and Blanchard, J.S. (2009). The 1.9 A structure of the branched-chain amino-acid transaminase (IlvE) from *Mycobacterium tuberculosis*. Acta Crystallogr. Sect. F Struct. Biol. Cryst. Commun. *65*, 1071–1077.

Tullius, M.V., Harth, G., and Horwitz, M.A. (2003). Glutamine synthetase GlnA1 is essential for growth of *Mycobacterium tuberculosis* in human THP-1 macrophages and guinea pigs. Infect. Immun. *71*, 3927–3936.

Ventura, M., Rieck, B., Boldrin, F., Degiacomi, G., Bellinzoni, M., Barilone, N., Alzaidi, F., Alzari, P.M., Manganelli, R., and O'Hare, H.M. (2013). GarA is an essential regulator of metabolism in *Mycobacterium tuberculosis*. Mol. Microbiol. *90*, 356–366.

Viljoen, A.J., Kirsten, C.J., Baker, B., van Helden, P.D., and Wiid, I.J. (2013). The role of glutamine oxoglutarate aminotransferase and glutamate dehydrogenase in nitrogen metabolism in Mycobacterium bovis BCG. PLoS ONE *8*, e84452.

Warner, D.F. (2014). *Mycobacterium tuberculosis* metabolism. Cold Spring Harb. Perspect. Med. *5*, a021121.

Weitzel, M., Nöh, K., Dalman, T., Niedenführ, S., Stute, B., and Wiechert, W. (2013). 13CFLUX2–high-performance software suite for $^{(13)}$C-metabolic flux analysis. Bioinformatics *29*, 143–145.

Wietzerbin-Falszpan, J., Das, B.C., Gros, C., Petit, J.F., and Lederer, E. (1973). The amino acids of the cell wall of *Mycobacterium tuberculosis* var. bovis, strain BCG. Presence of a poly(L-glutamic acid). Eur. J. Biochem. *32*, 525–532.

WHO (2018). Global Tuberculosis Report 2018 (World Health Organization).

Young, J.D. (2014). INCA: a computational platform for isotopically non-stationary metabolic flux analysis. Bioinformatics *30*, 1333–1335.

Zhang, J., Pavlova, N.N., and Thompson, C.B. (2017). Cancer cell metabolism: the essential role of the nonessential amino acid, glutamine. EMBO J. *36*, 1302–1315.

Zhao, Y., Butler, E.B., and Tan, M. (2013). Targeting cellular metabolism to improve cancer therapeutics. Cell Death Dis. *4*, e532.

Zimmermann, M., Kogadeeva, M., Gengenbacher, M., McEwen, G., Mollenkopf, H.J., Zamboni, N., Kaufmann, S.H.E., and Sauer, U. (2017). Integration of metabolomics and transcriptomics reveals a complex diet of *Mycobacterium tuberculosis* during early macrophage infection. mSystems *2*, e00057-17.

Zumla, A., George, A., Sharma, V., and Herbert, N.; Baroness Masham of Ilton (2013). WHO's 2013 global report on tuberculosis: successes, threats, and opportunities. Lancet *382*, 1765–1767.

STAR★METHODS

KEY RESOURCES TABLE

REAGENT or RESOURCE	SOURCE	IDENTIFIER
Bacterial Strains		
Mycobacterium tuberculosis H37Rv	Beste et al., 2013	N/A
Mycobacterium tuberculosis Δ*serC* H37Rv	This work	N/A
Mycobacterium tuberculosis Δ*serC*::SERC	This work	N/A
Escherichia coli DH5α	Beste et al., 2011	N/A
Experimental Models: Cell Lines		
THP-1 human monocytic cell line	Beste et al., 2013	ATCC TIB-202
Chemicals, Peptides and Recombinant Proteins		
Middle brook7H11 agar	Sigma-Aldrich	M0428-500G
Middlebrook 7H9	Sigma-Aldrich	M0178-500G
Oleic acid-albumin-dextrose-catalase enrichment supplement-500ml	Becton Dickenson	212351 (4312351)
Rosins minimal media	Beste et al., 2011	N/A
Luria-Bertani (LB) medium	Sigma-Aldrich	L3027-250G
Glycerol	Sigma-Aldrich	G7893-1L
Tyloxapol	Sigma-Aldrich	T8761-50G
Fetal calf serum	Sigma-Aldrich	F9665-500ML
RPMI medium 1640	Sigma-Aldrich	R0883
$^{15}N_1$ aspartic acid	Sigma-Aldrich	332135-100MG
$^{15}N_1$ leucine	Sigma-Aldrich	340960-500MG
$^{15}N_1$ glycine	Sigma-Aldrich	299294-250MG
$^{15}N_2$ glutamine	Sigma-Aldrich	490032-250MG
$^{15}N_1$ glutamic acid	Sigma-Aldrich	332143-100MG
$^{15}N_1$ alanine	Sigma-Aldrich	332127-500MG
L-glutamine	Sigma-Aldrich	G7513-100ML
Hydrochloric acid	Sigma-Aldrich	258148-500ML
Phorbol 12-myristate 13-acetate	Sigma-Aldrich	P8139-1MG
Phosphate buffer saline (PBS)	Sigma-Aldrich	D8537-500ML
NH_4Cl	Sigma-Aldrich	299251-20G
tert-butyldimethyl silyl chloride (TBDMSCl)	Sigma-Aldrich	00942-10ML
Gigapack III Plus Packaging Extract	Agilent Technologies	200204
L-Serine	Sigma-Aldrich	S4500
Q5 High-Fidelity 2X Master Mix	New England Biolabs	M0492S
$^{15}N_1$-serine	Sigma-Aldrich	609005-500MG
Software and Algorithms		
Isotopomer Network Compartmental Analysis (INCA)	Young, 2014	N/A
Metalign	Lommen, 2009	N/A
13CFLUX2	Weitzel et al., 2013	N/A
Omix	Omix Vizualization GmbH & Co. KG	
Chemstation	Agilent Technologies	N/A
Integrative Genomics Viewer	University of California	N/A
Snap Gene viewer	GSL Biotech LLC	N/A
Graph Pad Prism 8.0	GraphPad Software	N/A
MATLAB	The MathWorks, Inc	N/A

(*Continued on next page*)

Continued

REAGENT or RESOURCE	SOURCE	IDENTIFIER
NCBI Primer Blast	NIH	N/A
Other		
Plasmid sequencing	Source Biosciences, UK	N/A
Whole genome sequencing	MicrobesNG, UK	N/A

LEAD CONTACT AND MATERIALS AVAILABILITY

Further information and request for resources should be directed to and will be fulfilled by the Lead Contact, Johnjoe McFadden (j.mcfadden@surrey.ac.uk). Plasmids and strains generated in this study are available from the Lead Contact with a completed Materials Transfer Agreement.

EXPERIMENTAL MODEL AND SUBJECT DETAILS

Sources of *Mycobacterium tuberculosis, E. coli and* cell lines used for this study are reported in the Key Resources Table.

METHOD DETAILS

Mycobacterium tuberculosis (Mtb) cultivation

Mtb, H37Rv was cultivated on Middle brook7H11 agar and Middlebrook 7H9 broth with 5% (v/v) oleic acid-albumin-dextrose-catalase enrichment supplement and 0.5% (v/v) glycerol. Roisins minimal media was prepared with the composition described in Beste et al. (2011) and supplemented with 0.5% glycerol (v/v) as the carbon source and 10mM NH_4Cl as nitrogen source, 0.1% tyloxapol (v/v) at 37°C with agitation (150 rpm).

THP-1 macrophage cultivation

The human monocytic THP-1 cell line was grown in RPMI 1640 medium supplemented with 10% heat inactivated fetal calf serum at 37°C, 5% CO_2 and 95% humidity. For ^{15}N labeling experiments, modified RPMI supplemented with 0.2mM L-glutamine was used for testing $^{15}N_1$ aspartic acid and $^{15}N_1$ glutamic acid.RPMI without L-glutamine was used for testing $^{15}N_2$ glutamine (sigma). RPMI-1640 with 200 mM L-glutamine was used for testing $^{15}N_1$ leucine, $^{15}N_1$ ala and $^{15}N_1$ glycine.

^{15}N isotopic labeling during infection of macrophages with Mtb

For infection, THP-1 cells and Mtb cultures were prepared as described in Beste et al., 2013. THP-1 cells (3×10^7) were differentiated into macrophages for 3 days using 50 nM Phorbol 12-myristate 13-acetate in a 175 cm^2 tissue culture flasks. Macrophages were washed with warm PBS supplemented with 0.49 mM Mg^{2+} and 0.68 mM Ca^{2+} (PBS^+) and 30 mL of RPMI media was added. Mtb was grown in 7H9 broth for a week to an optical density of 1 (1×10^8 colony forming units per ml). Mtb cultures were washed 3 times with PBS and resuspended in RPMI media and added to the macrophages at a multiplicity of infection- 5. Each amino acid tracer except for $^{15}N_2$ glutamine was then added to the Mtb-infected macrophages at 3 times the concentration of that unlabelled amino acid present in the RPMI. For $^{15}N_2$ glutamine experiment, RPMI without unlabelled glutamine was used, because a large amount of unlabelled glutamine was present in RPMI as compared to other amino acids. To reduce the costs of the $^{15}N_2$ glutamine labeling experiment, the only glutamine in this RPMI was the tracer itself, added at 1 mM concentration which previously demonstrated by Tullius et al., 2003 and also confirmed in this study to have no detrimental effect on the macrophages (data not shown). The final concentration of tracers added during infection were- 0.6 mM $^{15}N_1$ aspartic acid, 0.53 mM $^{15}N_1$ glutamic acid, 0.8 mM $^{15}N_1$ leucine, 0.3 mM $^{15}N_1$ alanine, 1 mM $^{15}N_2$ glutamine and 0.4 mM $^{15}N_1$ glycine. Mtb infected macrophages were incubated for 3-4 h at 37°C, 5% CO_2 and 95% humidity. After incubation, macrophages were washed 3 times with PBS, tracers were added and left for 48 h at 37°C, 5% CO_2 and 95% humidity. After incubation for 48 h, macrophages were washed with cold PBS and Mtb cultures were harvested from macrophages using differential centrifugation (Beste et al., 2013). Amino acid hydrolysates were prepared from macrophage and Mtb using 6 M hydrochloric acid and incubation at 100°C for 24 h. The validity of the method for labeled amino acid extraction from intracellular Mtb was confirmed by comparing the nitrogen assimilation pattern obtained in RPMI grown labeled Mtb (control) (Figure S1, II). The control was set up by washing Mtb cultures with PBS and resuspending in RPMI for 48 h with equal amounts of ^{15}N isotope tracers that was previously used for infection assays. After 48 h, Mtb in RPMI were harvested followed preparation of amino acid hydrolysate.

In vitro ^{15}N isotopic labeling

Mtb was grown in Roisins minimal spiked with ^{15}N isotope tracers and left for 48 h at 37°C and cultures were agitated at 150 rpm. After 48 h, Mtb cultures were washed with triton, PBS and RIPA buffer. Cultures were harvested and amino acid hydrolysate was prepared by boiling Mtb in 6M hydrochloric acid for 24 h.

Gas-chromatography mass spectrometry (GC-MS) and ^{15}N mass isotopomer analysis

Amino acid hydrolysates were dried and derivatized using pyridine and tert-butyldimethyl silyl chloride (TBDMSCl) (sigma) (Rossi et al., 2017; Masakapalli et al., 2013). Amino acids were analyzed using a VF-5ms inert 5% phenyl-methyl column (Agilent Technologies) on a GC-MS system. MS data were extracted using chemstation GC-MS software and were baseline corrected using Metalign (Lommen, 2009). Mass data were corrected for natural isotope effects using Isotopomer network compartmental analysis (INCA) platform (Young, 2014). Average ^{15}N in an amino acid was calculated from the fractional abundance of the mass isotopomer in the entire fragment. For this study measurements > 1% were considered to be significantly enriched by the ^{15}N tracers.

Nitrogen network model (of Mtb)

A nitrogen transition model was set up for Mtb using information available in databases (KEGG, BioCyc, Tuberculist) and literature. The network model comprises the amino acid biosynthesis pathways of all 20 proteinogenic amino acids, as well as a simplified nucleotide biosynthesis formulation. Reaction reversibilities and requirements for growth were taken from Beste et al. (2011). For 20 protein-derived amino acids unidirectional uptake reactions were formulated while it was assumed that no backflow of nitrogen from Mtb to the phagosome exists. The mass isotopomers observed in the macrophage were deconvolved into distributions of isotopomer species and modeled by additional reactions (Figure S4). For comparability of the inference results across different nitrogen uptake constellations, flux values were formulated relative to the biomass synthesis rate. In total, the model has 98 independent fluxes, from which 50 are intracellular (40 net, 10 exchange) and 48 nuisance fluxes for modeling the deconvolution of the substrate species. This nitrogen transition template model was then duplicated per dataset to give rise to a sextuple model (Beyß et al., 2019), where each sub-model shared flux values, biomass requirements, and growth rate. Eventually, the sextuple model had 338 free fluxes (50 intracellular and 288 nuisance fluxes) that had to be inferred from 264 independent labeling measurements (15 measurement groups for Mtb and the host, respectively (Data S2; Figure S4).

^{15}N Flux Spectral Range Analysis (^{15}N-FSRA)

^{15}N-FSRA borrows the concept of parallel data integration from COMPLETE-MFA (Leighty and Antoniewicz, 2013) which, however, was reformulated resigning the knowledge of the experimentally inaccessible specific amino acid uptake rates and amending the traditional least-squares fitting approach by a tailored regularization approach to punish model complexity. In short, a penalty term was added to the weighted least-squares functional

$$\min_{\boldsymbol{v}} \|\boldsymbol{y}^{\boldsymbol{meas}} - \boldsymbol{y}^{\boldsymbol{sim}}\|_{\Sigma}^{2} + \lambda_1 \|\boldsymbol{v}\|_1 + \lambda_2 \|\boldsymbol{v}\|_2^2 \quad (1)$$

where $\boldsymbol{v}$ are the (independent) fluxes, $\boldsymbol{y}^{\boldsymbol{meas}}, \boldsymbol{y}^{\boldsymbol{sim}}$ the measured/simulated data, Σ the measurement covariance matrix, and $\lambda_{\boldsymbol{i}}, \boldsymbol{i} = 1, 2$ regularization parameters punishing non-zero flux values ($\lambda_1 = 10.0$ and $\lambda_2 = 0.1$).

A multi-start optimization strategy was applied to safeguard against local minima while solving Equation (1). The flux fitting procedure was performed with the high-performance simulator 13CFLUX2 (Weitzel et al., 2013) using the multifitfluxes module with 1,000 randomly sampled starting points and the NAG C optimization library (Version 6.23, Oxford, UK) with a maximum number of 250 iterations. From the 1,000 runs, those with residuals less than a cut-off of 203.5 were accepted (the overall optimal residual value was 182.01, corresponding to a χ^2 value > 99.99%, Data S3 and S4). This resulted in 800 accepted fits. From these accepted estimated flux distributions, FSRs (minimum, maximum, median) for each flux were derived (Table 1). Histograms of all FSRs are available in supplemental data file S4.

Construction of serC (Rv0884c) knockout strain of H37Rv

The knockout (KO) strain Δ*serC* was constructed using the bacteriophage mediated transduction of wild-type H37Rv (Bardarov et al., 2002). The strains and plasmid and primers used for this work are listed in Table S1A, B. Briefly, the allelic exchange vector was constructed by cloning upstream and downstream flanking regions of *serC* gene into the cosmid vector pYUB854with res sites flanking the hygromycin resistance (HYG^{R}) gene. The recombinant cosmid with the allelic exchange substrates was cloned into the *Pac*I site of the temperature sensitive shuttle phasmid phAEB159 using an *in vitro* λ-packaging reaction (GIGA PackII). The mycobacteriophage containing the recombinant pYUB854 was used for transduction of H37Rv. Bacterial cultures were grown up to exponential phase and washed with pre-warmed 7H9 no tween at 37°C. Phage was added at an m.o.i of 10 and incubated at 37°C for 4 h. After infection, cells were spun and plated onto 7H11 agar plates containing 100 μg ml^{-1} hygromycin and 50 μg ml^{-1} L-serine. Plates were incubated for 3 weeks and single colonies were picked for mutant screening. The knockout strain was confirmed by whole genome sequencing analysis where *serC* gene was deleted in H37Rv (Figure S6A, S6B; Data S5).

Construction of the complement strain ΔserC::SERC H37Rv

The complement strain was constructed using the integrating shuttle plasmid pMV361 with *hsp60* promoter *E. coli* origin of replication (oriE), the attP and int genes of mycobacteriophage L5 (for integration in the mycobacterial chromosome) and a kanamycin resistance gene (Kan^r) (Stover et al., 1991). *serC* was amplified using wild-type H437Rv genomic DNA as the template and primers with *EcoR*I and *Hind*III restriction site (Table S1). The amplified fragment was cloned into pMV361 *EcoR*I and *Hind*III sites downstream of the *hsp60* promoter. The recombinant plasmid was transformed into *E. coli* DH5α competent cells and plated onto LB agar containing 50 μg ml^{-1} kanamycin. Transformants were confirmed by digestion of the pMV361*serC* construct with *EcoR*I and *Hind*III. The construct was electroporated into the KO strain Δ*serC* and plated onto 7H11 agar plates containing 100 μg ml^{-1} hygromycin and 25 μg ml^{-1} kanamycin. Plates were incubated for 3 weeks and single colonies were picked for complement strain screening. Genomic DNA of the complement strain was isolated and the fragment containing *hsp60* promoter and *serC* gene was amplified. The complement strain had a PCR product of size 923 kb, identical to that of the construct pMV361*serC* confirming the complementation of the KO strain Figure S7B.

Growth of ΔserC and ΔserC::SERC H37Rv strains

For cultivation in agar plates, strains were grown in 7H11 agar supplemented with OADC. For Δ*serC* L-serine was added to the 7H11 + OADC plates at a concentration of 5mM and hygromycin at 100 μg ml^{-1}. For Δ*serC*::SERC H37Rv, kanamycin was added at 25 μg ml^{-1} to the 7H11 + OADC plates. For liquid cultures, strains were grown in 7H9 medium with OADC. To test for auxotrophy, Δ*serC* was grown in 7H9 with and without 5mM L-serine. WT and complement was grown in parallel in 7H9 medium with and without serine for comparison with the mutant.

Macrophage infections with WT, ΔserC and ΔserC::SERC H37Rv strains

THP-1 macrophages were cultivated as described in Beste et al. (2013) and 5 X 10^5 cells were seeded for each infection. WT, mutant and complement strains were added to the macrophages at an m.o.i of 0.1 for 4 h. After 4 h macrophages were washed and fresh RPMI medium with 10% FBS was added. Macrophage survivability upon infection with the strains was monitored using crystal violet assays during the period of infection (data not shown). For bacterial survivability test, macrophages were lysed with 0.1% Triton X-100 at specific time points- 0 (inoculum before infection of macrophage), day 1, day 3 and day 7, and plated on 7H11 agar plates with OADC. 7H11 plates for Δ*serC* strain were supplemented with 5mM serine and hygromycin was added at 100 μg ml^{-1}, and for Δ*serC*::SERC strain, kanamycin was added at 25 μg ml^{-1}. Plates were incubated for 3 weeks at 37°C and colony forming unit ml^{-1} were recorded for the three strains.

$^{15}N_1$-serine isotopic labeling

Starter cultures of WT, mutant and complement strains were cultivated in 7H9 medium with OADC, 5mM L-serine and respective antibiotics for 4-5 days. For labeling experiments, starter cultures were spun and re-suspended Roisin's minimal medium containing glycerol and ammonium chloride as carbon and nitrogen sources respectively, and with 50 μg ml^{-1} $^{15}N_1$-serine. Cultures were incubated for 48 h at 37°C. After incubation, cultures were spun and amino acid hydrolysates were prepared as described previously. ^{15}N enrichment of amino acids was performed with GC-MS as described previously.

QUANTIFICATION AND STATISTICAL ANALYSIS

Statistical analyses were performed using Student's t test and significant differences were calculated using Holm Sidak method in graph pad prism 8.0. The details of number and type of replicate measurements used for calculating mean and standard error of the mean (SEM) are included in figure legends. Residual values for FSRA predictions (minimum, maximum, median) were calculated in 13CFLUX2 software and are described in details in the methods section.

DATA AND CODE AVAILABILITY

Data generated in this study are available in the supplemental items

Cell Reports, Volume *29*

Supplemental Information

Intracellular *Mycobacterium tuberculosis* Exploits Multiple Host Nitrogen Sources during Growth in Human Macrophages

Khushboo Borah, Martin Beyß, Axel Theorell, Huihai Wu, Piyali Basu, Tom A. Mendum, Katharina NÖh, Dany J.V. Beste, and Johnjoe McFadden

Figure S1

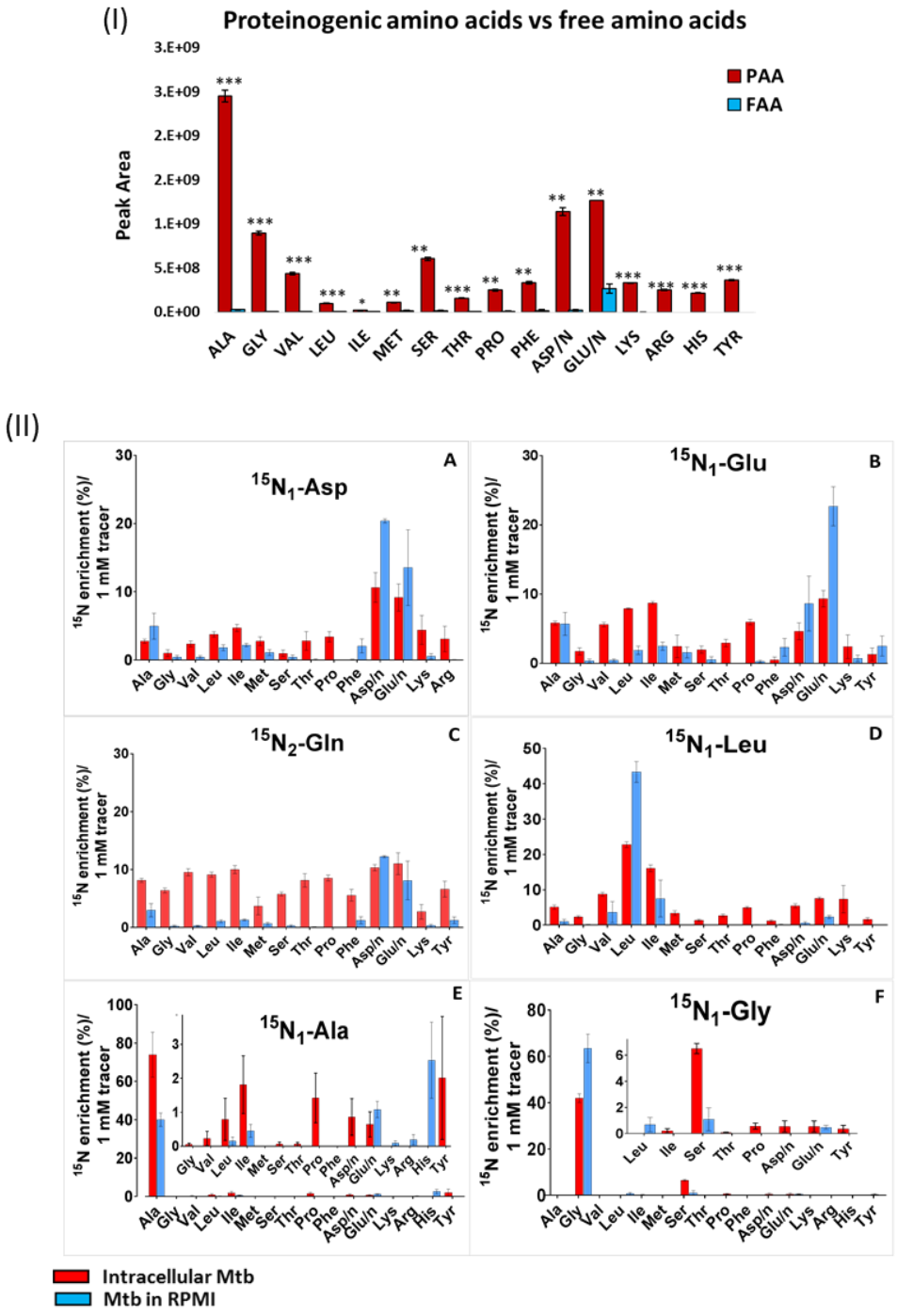

Figure S1 (I) **Relative abundance of free and proteinogenic amino acids in Mtb, Related STAR Methods**. Amino acids- free and proteinogenic were harvested by quenching Mtb cells in methanol:chloroform (2:1), followed by polar/non-polar biphasic separation of free (FAA) amino acids and proteinogenic amino acids (PAA). Free amino acids in the polar phase were dried for GC-MS analysis and proteinogenic amino acids in the non-polar phase were isolated by centrifugation and hydrolysed in 6M HCl, followed by GC-MS analysis. Values are mean ± SEM from 2 technical replicates. Statistical significance, * $P < 0.05$; **, $p < 0.005$; *** $P < 0.0005$. (II) **^{15}N enrichment of amino acids measured in intracellular Mtb and RPMI grown Mtb (control), Related to Figure 1, STAR Methods**. Measurements for intracellular Mtb and RPMI grown Mtb were obtained from experiments using tracers- $^{15}N_1$-Asp (A), $^{15}N_1$-Glu (B), $^{15}N_2$-Gln (C), $^{15}N_1$-Leu (D), $^{15}N_1$-Ala (E) and

$^{15}N_1$-Gly (F). Enrichments were measured ((normalized for each 1mM tracer) in the protein-derived amino acids of intracellular Mtb and RPMI grown Mtb following incubation with the tracers for 48 h. Values are mean ± SEM from 3-8 biological replicates for intracellular Mtb and from 3 biological replicates for RPMI grown Mtb respectively.

Figure S2

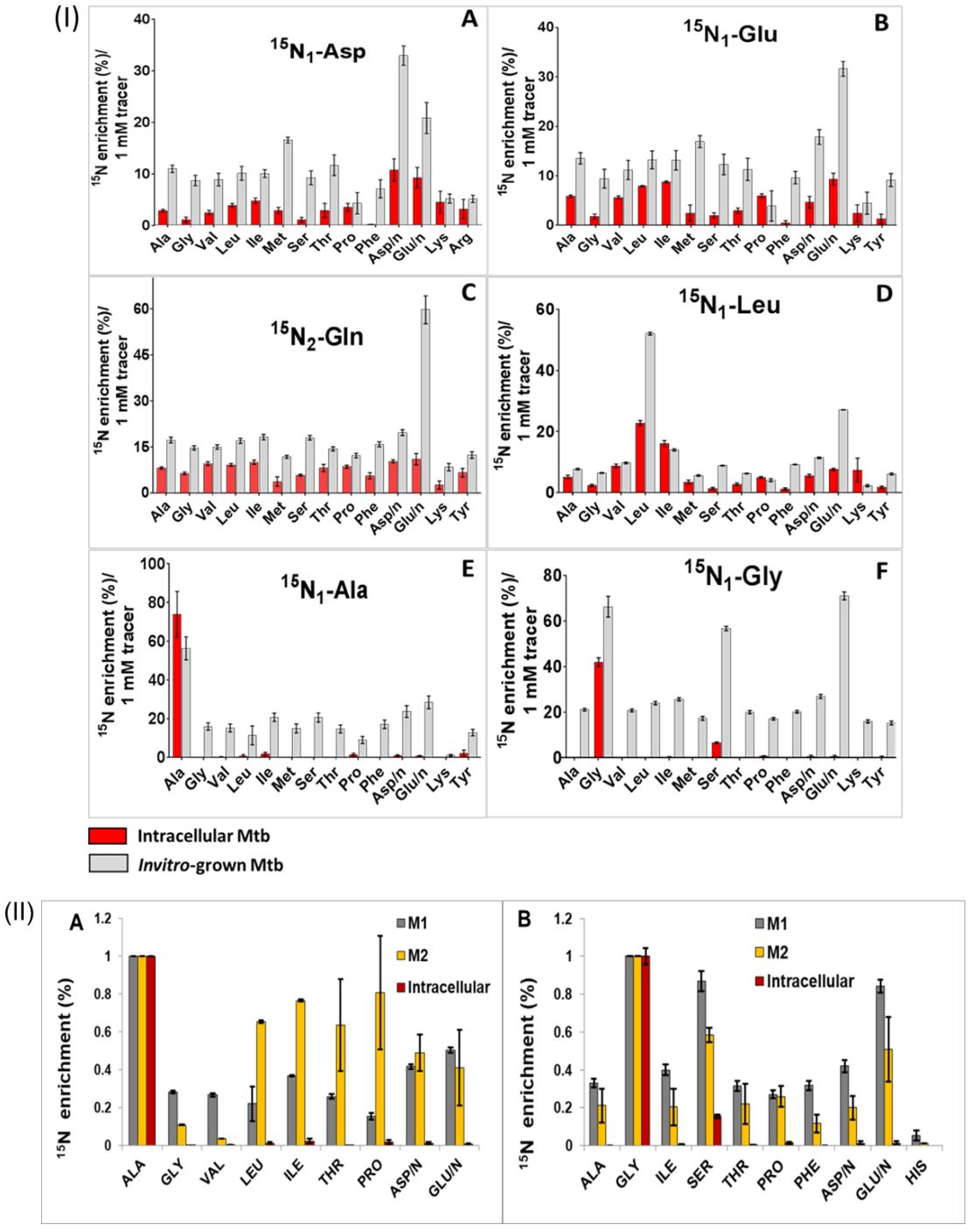

Figure S2. (I) **^{15}N enrichment of amino acids measured in intracellular Mtb and *in vitro*-grown Mtb, Related to Fig. 1**. Data is shown for intracellular Mtb and *in vitro*-grown Mtb in Roisins minimal media following 48 h incubation with each of the tracers $^{15}N_1$-Asp (A), $^{15}N_1$-Glu (B), $^{15}N_2$-Gln (C), $^{15}N_1$-Leu (D), $^{15}N_1$-Ala (E) and $^{15}N_1$-Gly (F). After incubation, enrichments were measured (normalized for

each 1mM tracer) in the protein-derived amino acids of intracellular Mtb isolated from the macrophage and from Mtb incubated in RPMI. Values are mean ± SEM from 3-8 biological replicates for intracellular Mtb and from 3 biological replicates for *in vitro*-grown Mtb respectively. (II) **Comparison of amino acid extraction methods M1 vs M2 from *in vitro*-grown Mtb, Related to Figure 1, STAR Methods**. M1- the original method used in the manuscript to obtain measurements in Fig. 1D and M2 is the method followed exactly like for the amino acid harvest from intracellular Mtb (Fig. 1A) with extensive washing. We performed quantitative comparisons of M1, M2 with the intracellular data (Fig. 1A). Fractional labelling was compared for the two amino acid tracers $^{15}N_1$-ALA (A) and $^{15}N_1$-GLY (B). The enrichments were normalized to the parent amino acid labels for quantitative comparisons across the three methods used for in vitro and intracellular Mtb. Students t-test and Holm-Sidak statistical analysis found no significant differences between the enrichment profiles measured with M1 and M2. Values are mean ± SEM from 3-8 biological replicates for intracellular Mtb and from 3 biological replicates for *in vitro*-grown Mtb respectively.

Figure S3

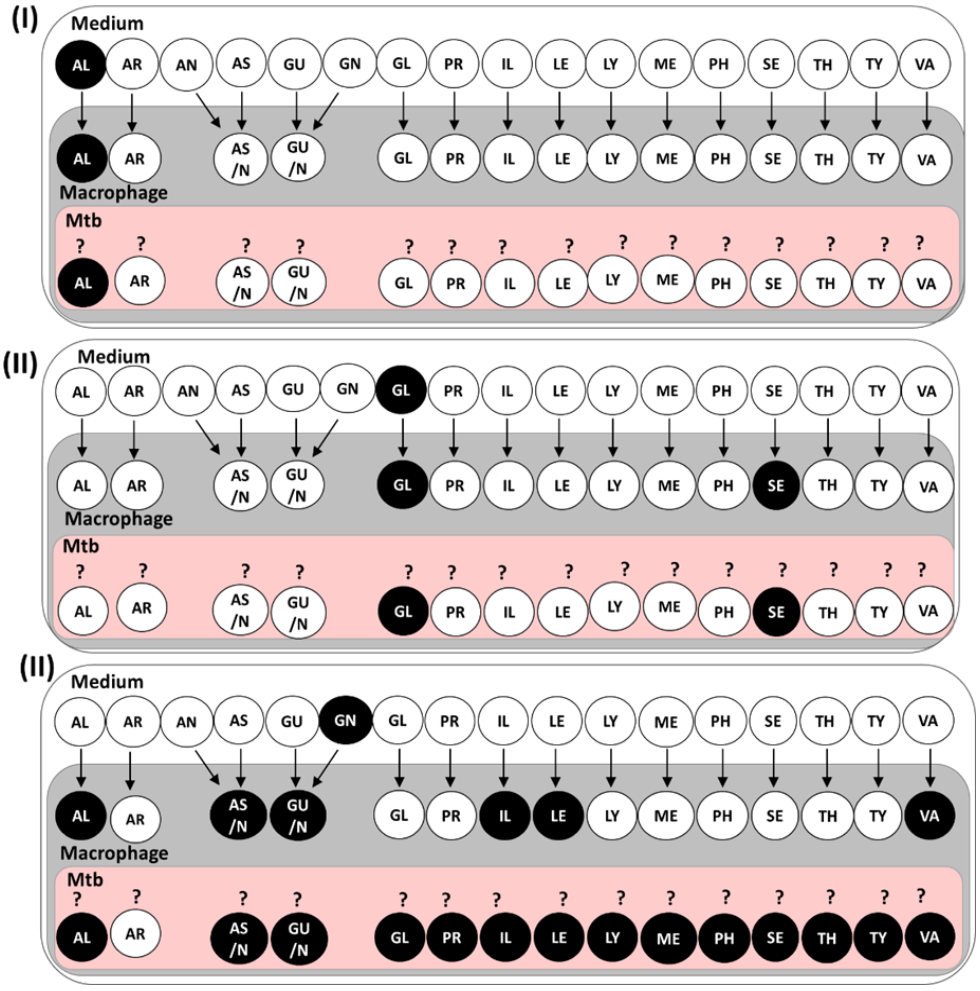

Figure S3. **Qualitative ^{15}N Labelling patterns of intracellular Mtb, infected macrophages and growth medium, Related to STAR Methods**. The pattern is shown for the tracers- $^{15}N_1$-Ala (I), $^{15}N_1$-Gly (II) and $^{15}N_2$-Gln (III). Labelled amino acids are filled in black and the unlabelled amino acids in white. Amino acids acquired directly from the medium by infected macrophage are indicated by arrows. The uncertainty of direct or indirect uptake of amino acids by Mtb from the macrophage is indicated by ?. Abbreviations for amino acids- AL (alanine), AR (arginine), AN (asparagine), AS (aspartate), AS/N (aspartate/asparagine), GU (glutamate), GN (glutamine), GU/N

(glutamate/glutamine), GL (glycine), PR (proline), IL (isoleucine), Le (leucine), LY (lysine), ME (methionine), PH (phenylalanine), SE (serine), TH (threonine), TY (tyrosine) and VA (valine).

Figure S4

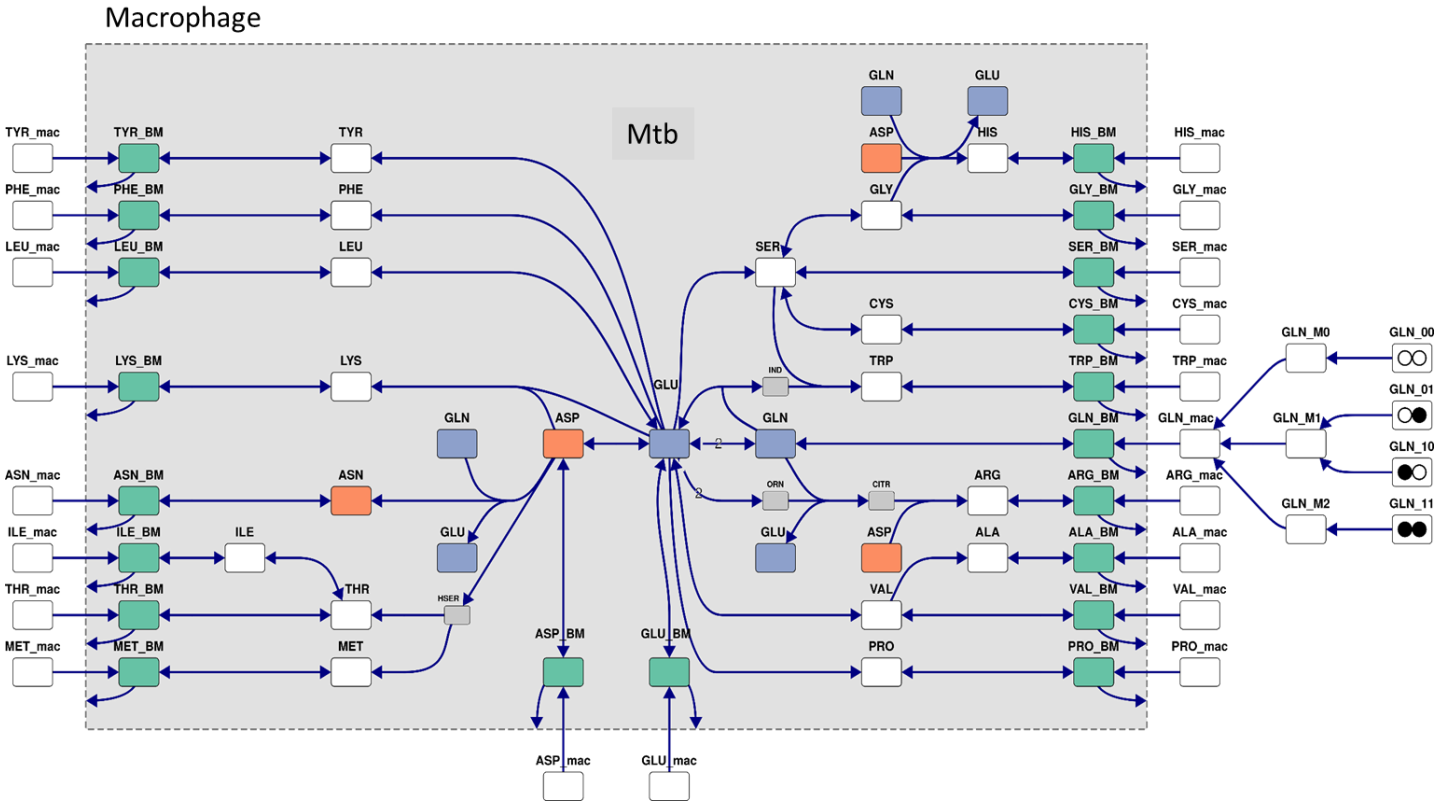

Figure S4. **^{15}N FSRA metabolic network of Mtb, Related to Figure 5 and Table 1.** Network model of nitrogen metabolism. On the right, the input pool deconvolution is shown for GLN (glutamine). Biomass pools are coloured in green. ASP/ASN and GLN/GLU pairs occur several times in the network and are coloured in red and blue, respectively. Grey coloured metabolites indicate intermediate pools. White boxes inside the MTB box code for *de novo* synthesized amino acids. The following abbreviations are used: CITR (citrulline), HSER (homoserine), IND (indole) and ORN (ornithine).

Figure S5

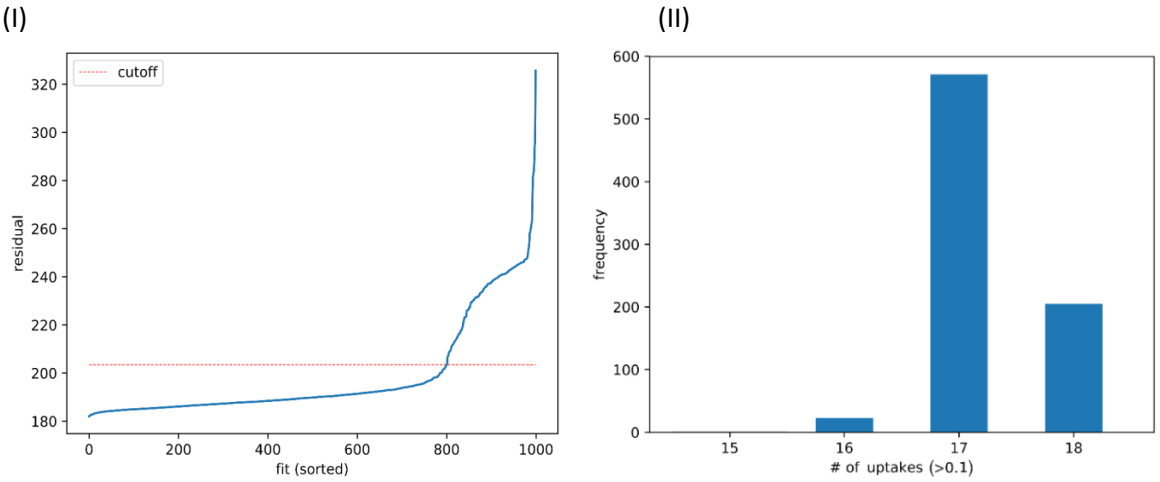

Figure S5. (**I) Residual values, Related to Table 1 and STAR Methods.** Residual values of 1,000 flux estimations sorted by size. Fits with residual values below the red line (cut-off=182.01) were accepted and used for interpretation. (II) **Histogram showing the total number of amino acids taken up from the macrophage, Related to Table 1 and STAR methods.**

Figure S6

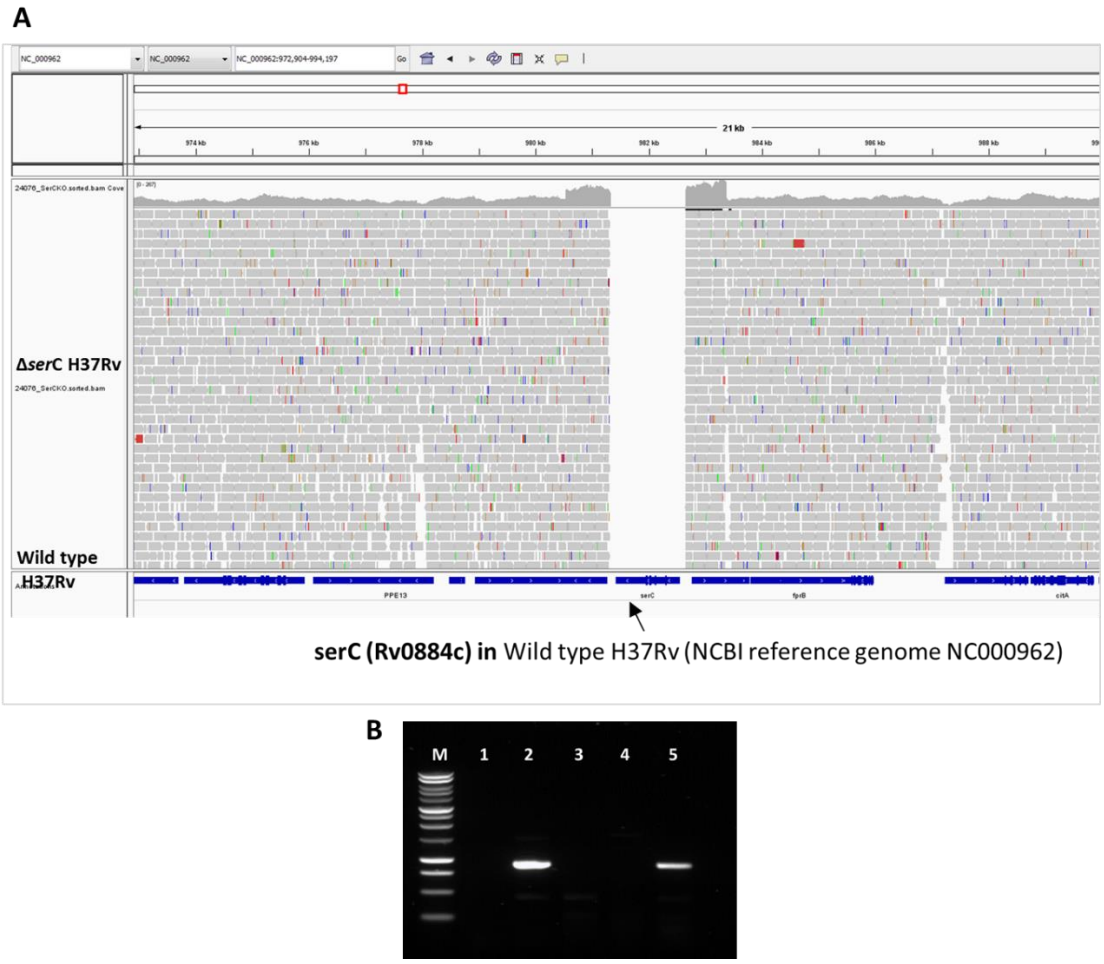

Figure S6. **Confirmation of Δ*serC* mutant and complement Δ*serC*::SERC strains, Related to STAR methods.** (A) Sequence comparisons between the wild type and Δ*serC* H37Rv strains using Artemis. The comparisons show a gap in *ser*C (Rv0884c) gene in the mutant strain confirming the deletion of the gene (Data file S5). (B) PCR analysis to confirm the complement Δ*serC*::SERC. 923kb PCR product of *hsp60* promoter and *serC* gene was amplified from the pMV361*serC* construct (lane 2) and Δ*ser*C::SERC genomic DNA (gDNA) (lane 5) confirming the complement to have the integrated construct pMV361*serC*. Marker-M, 1- water control, 2- pMV361*serC* plasmid, 3- WT H37Rv gDNA , 4- Δ*serC* H37Rv gDNA and 5- Δ*serC*::SERC H37Rv gDNA.

Table S1**. A- Strains and plasmids used for construction of Δ*serC* mutant and complement Δ*serC*::SERC strains, Related to STAR Methods. B- Primers used for construction of Δ*serC* mutant and complement Δ*serC*::SERC strains, Related to STAR methods.**

A

Strain	**Genotype and relevant characteristics**	**Reference or source**
Escherichia coli DH5α	Competent cells	Beste et al., 2013
E. coli HB101	F–, thi-1, hsdS20 (rB–, mB–), supE44, recA13, ara-14, leuB6, proA2, lacY1, galK2, rpsL20 (strr), xyl-5, mtl-1	Invitrogen
E. TOP10	Competent cells, HYG^R	Thermo Fisher Scientific
E. coli DH5α-pMV361*serC*	Strain harbouring pMV361*serC* construct, KAN^R	This work
M. smegmatis mc^2155	Easily transformable strain, used for phage preparation	Baradov et al., 2002
Plasmid		
pYUB854	Cosmid vector, with res sites flanking the HYG^R gene	Bardarov et al. 2002
pYUB854_LF	pYUB854 + 716 bp left flanking sequence of *serC* (Rv0884c)	This work
pYUB854_RF	pYUB854 + 787 bp right flanking sequence of *serC* (Rv0884c)	This work
pYUB854_LFRF-AES	pYUB854 + left and right flanking sequence of *serC* (Rv0884c)	This work
pMV361	*E. coli*-Mycobacteria shuttle vector, groEL2 (*hsp60*) promoter, KAN^R, OriM	Stover et al., 1991
pMV361*serC*	pMV361 containing serC (Rv0884c) gene, KAN^R	This work
Phage		
phAE159	Mycobacterial phage	Bardarov et al. 2002
phAE159:Δ*serC*	phAE159 + pYUB854_LFRF-AES, HYG^R	This work

B

Primer Sequences		
Gene/loci	**Forward primer (5'-3')**	**Reverse primer (5'-3')**
serC (Rv0884c) upstream (left flanking region), allelic exchange	GGTGGTCTTAAGATGATCGGATGCAGCGACTT	GGTGGTTCTAGACTGGTGGCTGGGTCATAGTG
serC (Rv0884c) downstream (right flanking region), allelic exchange	GGTGGTAAGCTTTAGAGTGCGCACGTAACAGG	GGTGGTACTAGTCACATCTTCCCAGGCAGGTA
serC (Rv0884c) PCR to construct pMV361*ser*C	GGTGGTGAATTCATGGCCGACCAGCTCAC	GGTGGTAAGCTTCTAAAGCCGCTCGACCACC
Δ*serC*::SERC confirmation PCR	ACATACTCACCCGGATCGGA	CGAAGTAGTAGGCGTCGGTC